SnowScat's tomographic profiling mode: a time series acquired during the ESA SnowLab campaign

O. Frey[1,2], C. L. Werner[1], R. Caduff[1], M. Schneebeli[3], A. Wiesmann[1]

[1] Gamma Remote Sensing AG
[2] ETH Zurich, Earth Observation and Remote Sensing
[3] WSL Institute for Snow and Avalanche Research SLF

New technologies (sensors/methods) II

Context



- SnowScat = a fully-polarimetric scatterometer originally designed to measure the radar cross-section of snow at a frequency range from 9.2 to 17.8 GHz (X-band to Ku-band) [1,2,3].
- SnowScat in original measurement mode in Sodankylä, Finland (Photo courtesy of ESA).

---

[1] A. Wiesmann, T. Strozzi, C. L. Werner, U. Wegmuller, and M. Santoro, "Microwave remote sensing of alpine snow", in *Proc. IEEE Int. Geosci. Remote Sens. Symp.*, Jul. 2007, pp. 1223–1227.

[2] C. L. Werner, A. Wiesmann, T. Strozzi, M. Schneebeli, and C. Matzler, "The SnowScat ground-based polarimetric scatterometer: Calibration and initial measurements from Davos Switzerland", in *Proc. IEEE Int. Geosci. Remote Sens. Symp.*, Jul. 2010, pp. 2363–2366.

[3] A. Wiesmann, C. L. Werner, T. Strozzi, C. Matzler, T. Nagler, H. Rott, M. Schneebeli, and U. Wegmuller, "SnowScat, X- to Ku-band scatterometer development", in *Proc. ESA Living Planet Symposium*, Jun. 2010.

Motivation for tomographic mode for SnowScat

- Tomographic extension aims at enhancing the SnowScat device to better respond to the recommendations made by ESA's Earth Science Advisory Committee (ESAC) on the deselected Earth Explorer 7 candidate CoReH2O.
- Such new capability should allow to perform high-resolution tomographic profiling observations to gain further insight into the complex electromagnetic interaction within snowpacks.
- Similar tomographic experiments have shown the potential of this type of measurement[4,5,6].

---

[4] S. Tebaldini and L. Ferro-Famil, "High resolution three-dimensional imaging of a snowpack from ground-based SAR data acquired at X and Ku band", in *Proc. IEEE Int. Geosci. Remote Sens. Symp.*, Jul. 2013, pp. 77–80.

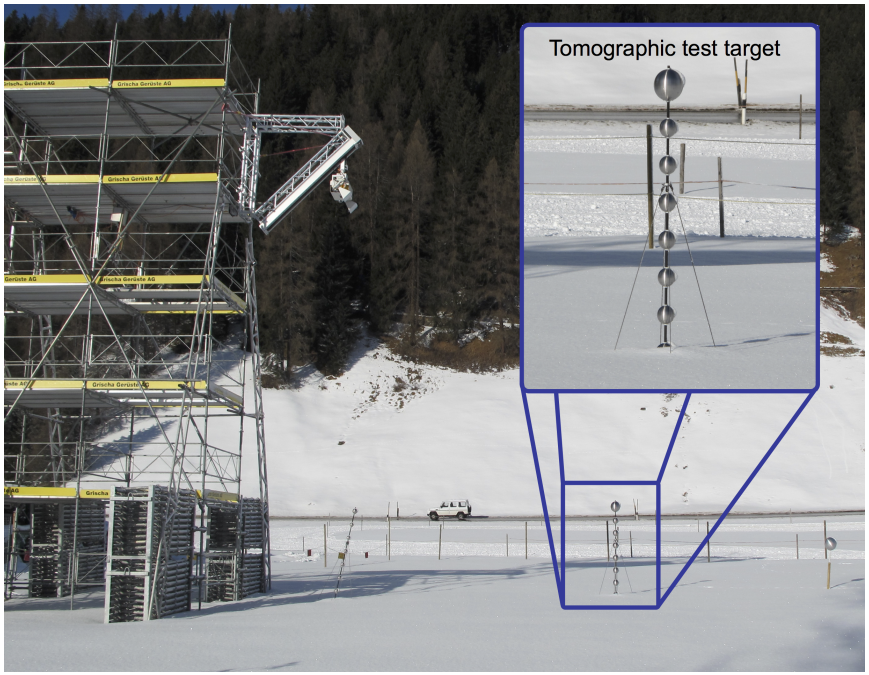
[5] L. Ferro-Famil, S. Tebaldini, M. Davy, and F. Boute, "3D SAR imaging of the snowpack at X- and Ku-band: Results from the AlpSAR campaign", in *Proc. of EUSAR 2014 - 10th European Conference on Synthetic Aperture Radar*, Jun. 2014, pp. 1–4.

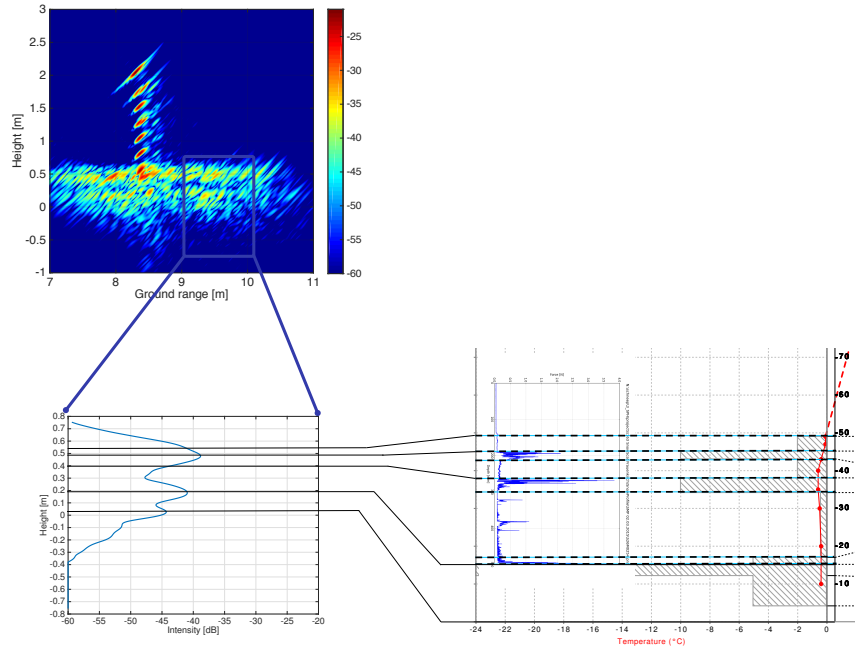
[6] K. Morrison and J. Bennett, "Tomographic profiling - a technique for multi-incidence-angle retrieval of the vertical SAR backscattering profiles of biogeophysical targets", *IEEE Trans. Geosci. Remote Sens.*, vol. 52, no. 2, pp. 1350–1355, Feb. 2014.

Content of this talk

1. SnowScat experimental setup at ESA SnowLab test sites.
2. SnowScat system/measurement principle and its new tomographic profiling capabilities.
   $\Rightarrow$ Synthetic aperture along elevation direction.
3. Tomographic processing scheme.
4. Vertical 2-D tomographic profiles (time series).
5. Co-polar & interferometric phase of 2-D tomo. profiles.
6. Refinement of tomo. processing. $\Rightarrow$ Estim. of refractive index.
7. Discussion / Outlook

First experimental proof of concept, Davos (CH), winter 2014/2015



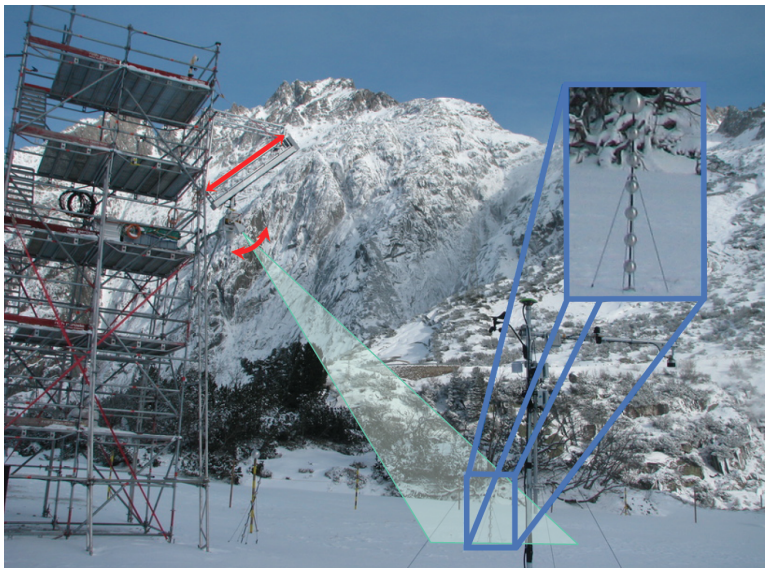


- Proof of concept after tomograph. hardware extension.
- Few measurements and less than 60cm snow accumulation. [7]

[7] O. Frey, C. L. Werner, and A. Wiesmann, "Tomographic profiling of the structure of a snow pack at X-/Ku-band using SnowScat in SAR mode", in *Proc. EuRAD 2015 - 12th European Radar Conference*, Sep. 2015, pp. 21–24.

ESA SnowLab experimental setup 2015/2016

Testsite Gerstenegg, Switzerland, hosted by KWO, Jan., 2016.





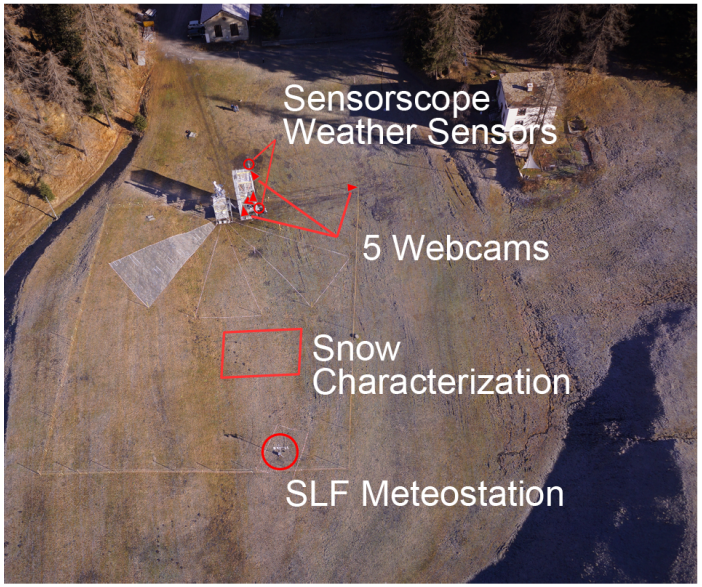


Aim:

- Collect time series of tomographic profiles of snow pack.
- Accompanied with some in-situ measurements (snow profiles, meteo param.)

ESA SnowLab experimental setup 2016/2017

Testsite Davos Laret, 1514 m a.s.l., hosted by SLF.



UAV-Image / Y. Bühler & M. Jaggi





Aim:

- 1 tomogram per day
- More extensive in-situ measurements (snow profiles, SWE, SMP, microCT, meteo param.)
- “Controlled” environment.

System specs. used in tomographic experiment

Frequency	SFCW from 9.2 to 17.8GHz
Incidence angle	-40^o to 110^o (used: 45^o)
Azimuth angle	-180^o to 180^o (used: 0^o)
Sampling spacing	0.04 m
Number of samples	50
Synth. aperture length	1.94 m
3dB res. (stripmap m.)	0.15 m
Power	230V, max $\sim$ 60W
Weight	$\sim$ 40 kg
Temperature range	-40^{o}C to 40^{o}C
Antennas	Dual pol, $<$ 10^o (3dB)
Antenna cross-pol	$<$ -25dB
Polarization	HH, HV, VV, VH
Dynamic range	Receiver dynamic range $>$ 80dB with the 16bit ADC
Signal bias	$<$ 0.5dB
Gain characterization	Internal calibration, calibration sphere (Ø = 25.4cm)
RFI	Frequency blacklist

Measurement principle of SnowScat (1)

- Stepped-frequency, continuous-wave (SFCW) radar
- Tuneable bandwidth, frequency steps, etc.
- Settings for tomographic profiling:

$$f_{start} = 9.199984 GHz$$

$$\Delta f = 6.144 MHz$$

$$n_{f.steps} = 1400$$

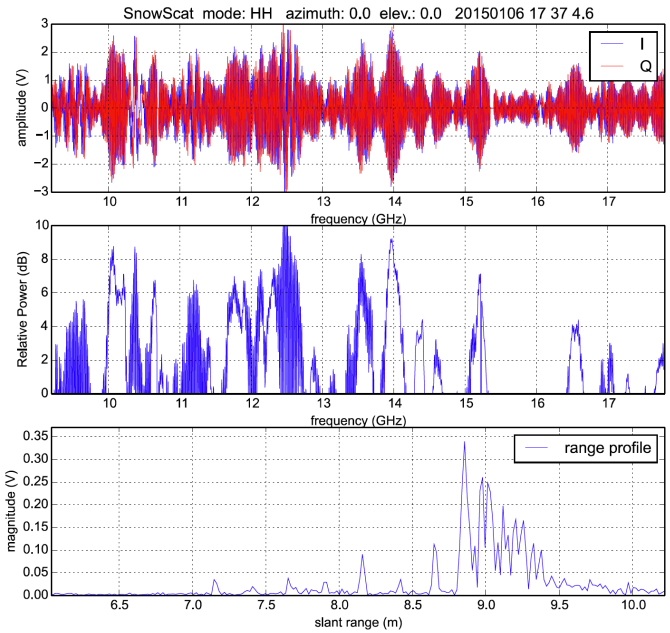
$$\rightarrow R_{unamb} = \frac{c}{2\Delta f} \approx 24.3 m$$

- Max. bandwidth:

$$B = n_{f.steps} \Delta f = 8.6016 GHz$$

- Nominal range resolution:

$$\rightarrow \delta R = \frac{c}{2B} = 1.73 cm\,!$$



- At each frequency step the scene is sampled with a narrow-bandwidth signal (25kHz).
- Range profile (I/Q) is obtained via:

$$s_r(t) = IFFT\{S_r(f)^*\}$$

- Repeated for each channel CC, HH, HV, VH, VV.

Measurement principle of SnowScat (2)

- Frequency blacklist is applied to prevent RFI.
- Omitted various bands at SnowLab site 2015/2016:

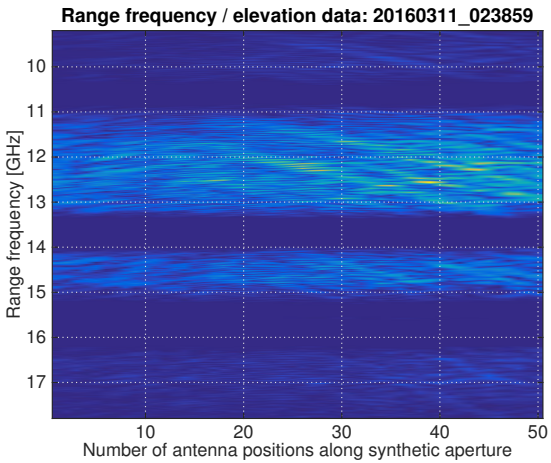
  10.60 - 10.68 GHz : Satellite radiometry and radio astronomy.

  10.68 - 10.70 GHz : Radio astronomy.

  13.40 - 14.00 GHz : FSS/ETS.

  15.35 - 15.40 GHz : Radio astronomy.

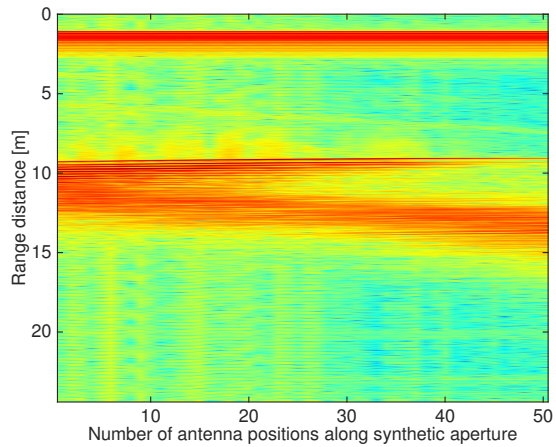
  15.77 - 16.13 GHz : MIL Radar.



  Loss of range resolution & higher sidelobes.

⇒ More complete frequency band in 2016/2017.

- Range-compressed data set obtained from a tomography scan.



- Essentially: a range-compressed SAR data set that requires an additional focusing step in elevation direction.

Tomographic processing scheme

Tomographic profiling by means of time-domain back-projection (TDBP)[9,10]:
- Focusing to a ground-range / height reconstruction grid.
- Taking into account strong range-cell migration due to short rel. range distance.
- Taking into account refraction through virtual range distance R_v.

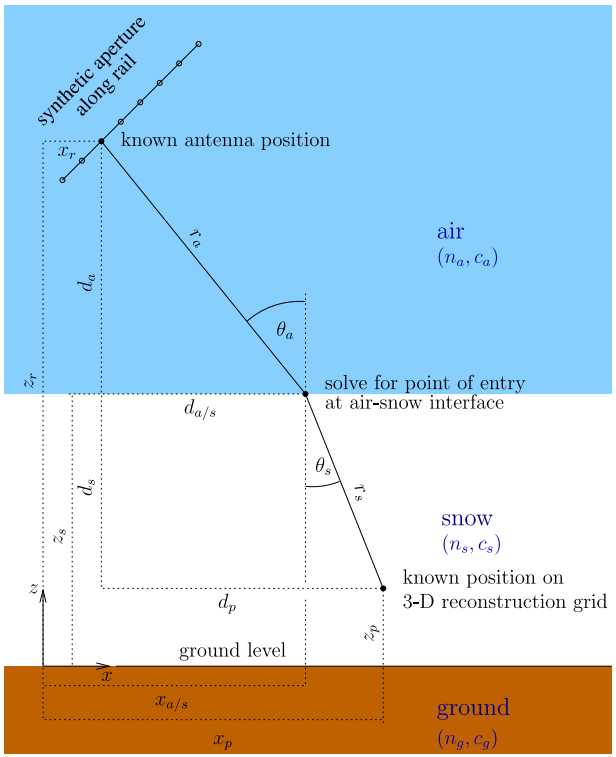
$$v(\vec{r}_i) = \sum_{k=1}^{M} g_k[R_v(\vec{r}_i, \vec{r}_k, n_s)] \cdot \exp[i\, 4\pi / \lambda R_v(\vec{r}_i, \vec{r}_k, n_s)] \,.$$

$\vec{r}_i$	: 3-D position vector of the target location for which the tomographic inversion is performed.
$\vec{r}_k$	: 3-D position vector of the antenna phase center at position k within the synthetic aperture.
$g_k(...)$	: Range-compressed signal at antenna position k.
λ	: Wavelength of the carrier signal.
$R_v(\vec{r}_i, \vec{r}_k, n_s)$	: (Virtual) range distance between antenna position k and the location $\vec{r}_i$ taking into account the refraction.
$v(\vec{r}_i)$	: Tomographically focused signal at location $\vec{r}_i$.

[9] O. Frey and E. Meier, "3-D time-domain SAR imaging of a forest using airborne multibaseline data at L- and P-bands", *IEEE Trans. Geosci. Remote Sens.*, vol. 49, no. 10, pp. 3660–3664, Oct. 2011.

[10] O. Frey, F. Morsdorf, and E. Meier, "Tomographic imaging of a forested area by airborne multi-baseline P-band SAR", , *Sensors, Special Issue on Synthetic Aperture Radar*, vol. 8, no. 9, D. Riccio, Ed., pp. 5884–5896, Sep. 2008.

Simplified refraction model



Calculation of the point of entry is based on the following trigonometric relationships.

$$\sin\theta_a = \frac{d_{a/s}}{\sqrt{d_{a/s}^2 + d_a^2}}, \quad \sin\theta_s = \frac{d_p - d_{a/s}}{\sqrt{(d_p - d_{a/s})^2 + d_s^2}}$$

and Snel's law :

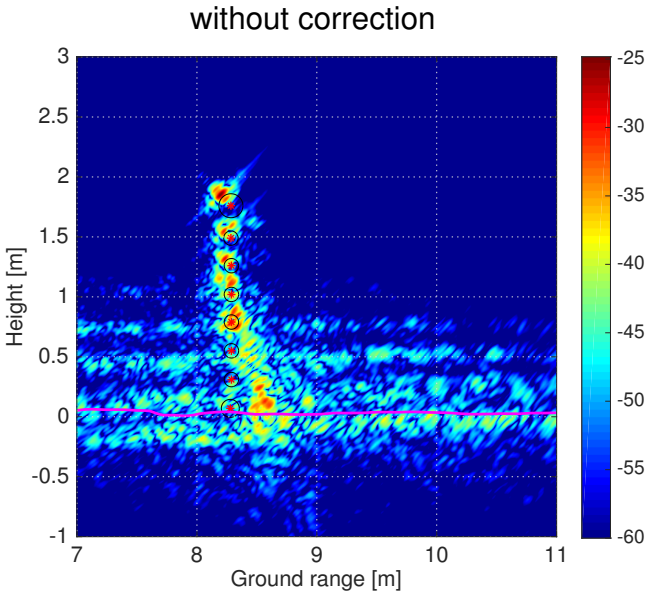
$$\frac{\sin\theta_a}{\sin\theta_s} = \frac{n_s}{n_a}$$

$$\Rightarrow \frac{d_p - d_{a/s}}{\sqrt{(d_p - d_{a/s})^2 + d_s^2}} - \frac{n_a}{n_s} \cdot \frac{d_{a/s}}{\sqrt{d_{a/s}^2 + d_a^2}} = 0$$

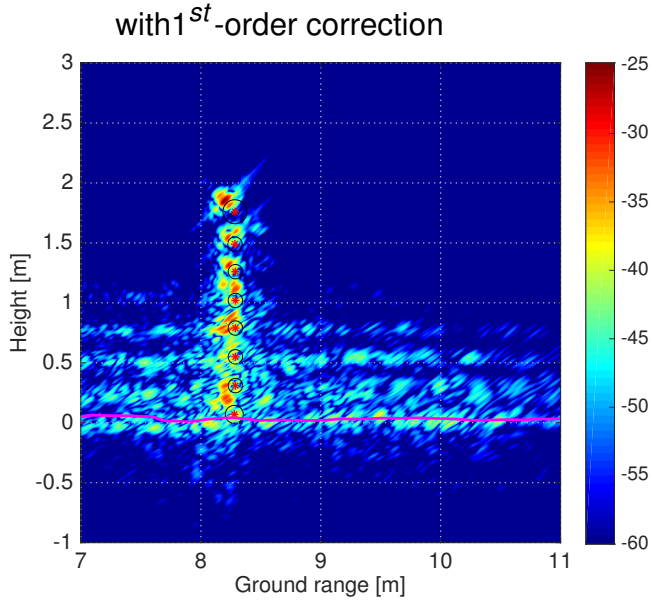
The virtual range distance R_v corresponding to the actual time delay in the radar echo is then:

$$R_v = n_a \sqrt{d_{a/s}^2 + d_a^2} + n_s \sqrt{(d_p - d_{a/s})^2 + d_s^2}. \quad (1)$$

Experimental results: tomographic profiles (1)



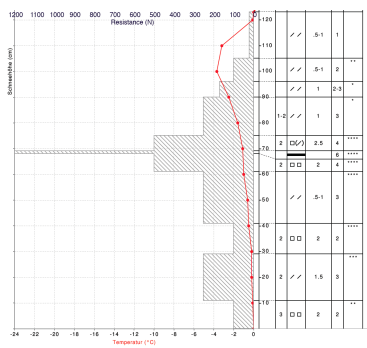
(e) 2016-03-11



(f) 2016-03-11

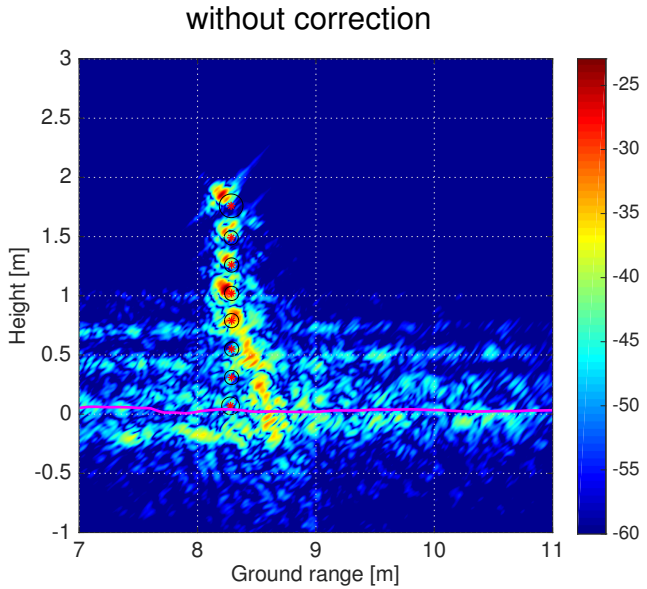


(g) 2016-03-11

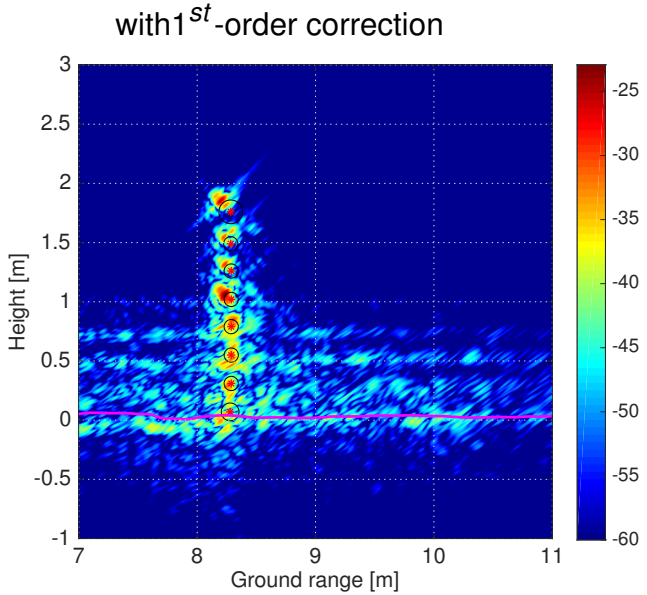


(h) 2016-03-11

Tomographic profiles (2)



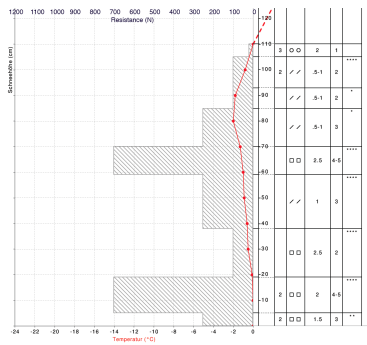
(i) 2016-03-18



(j) 2016-03-18

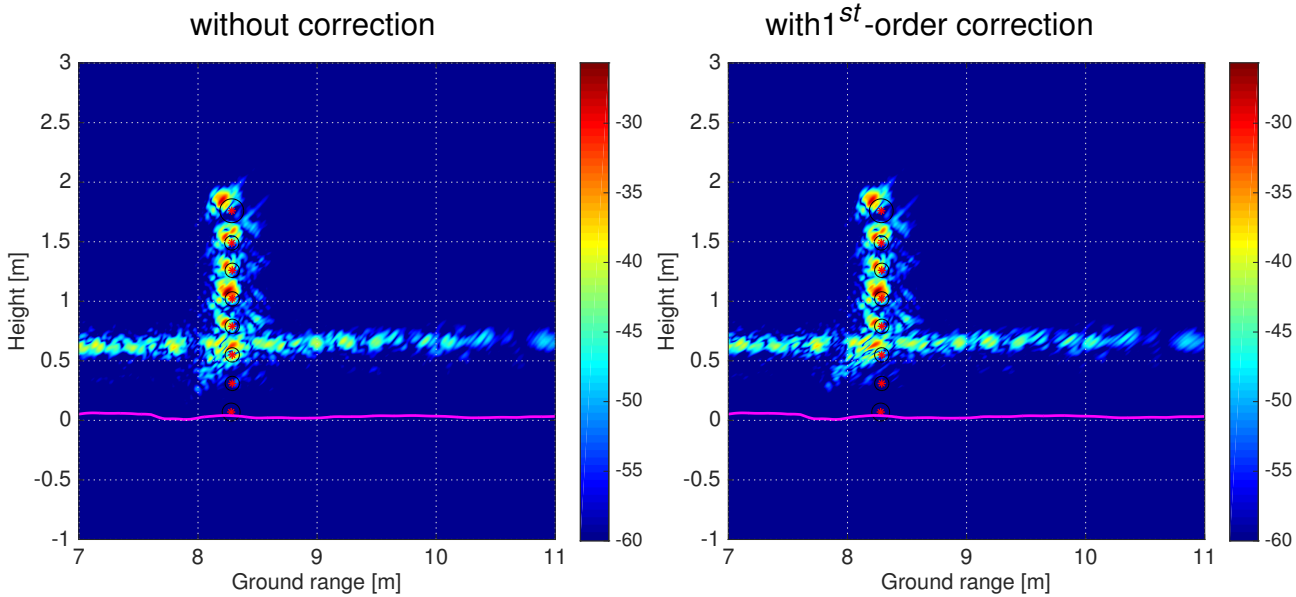


(k) 2016-03-18

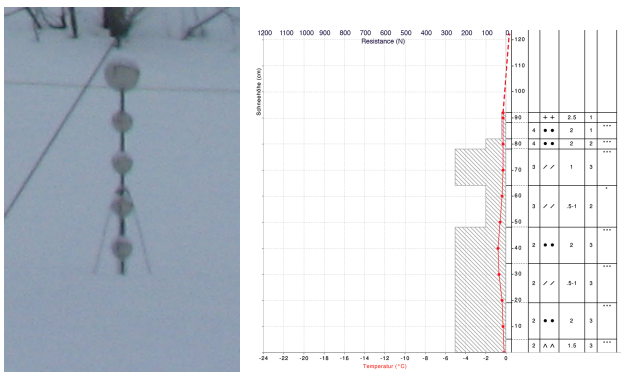


(l) 2016-03-18

Tomographic profiles (3)



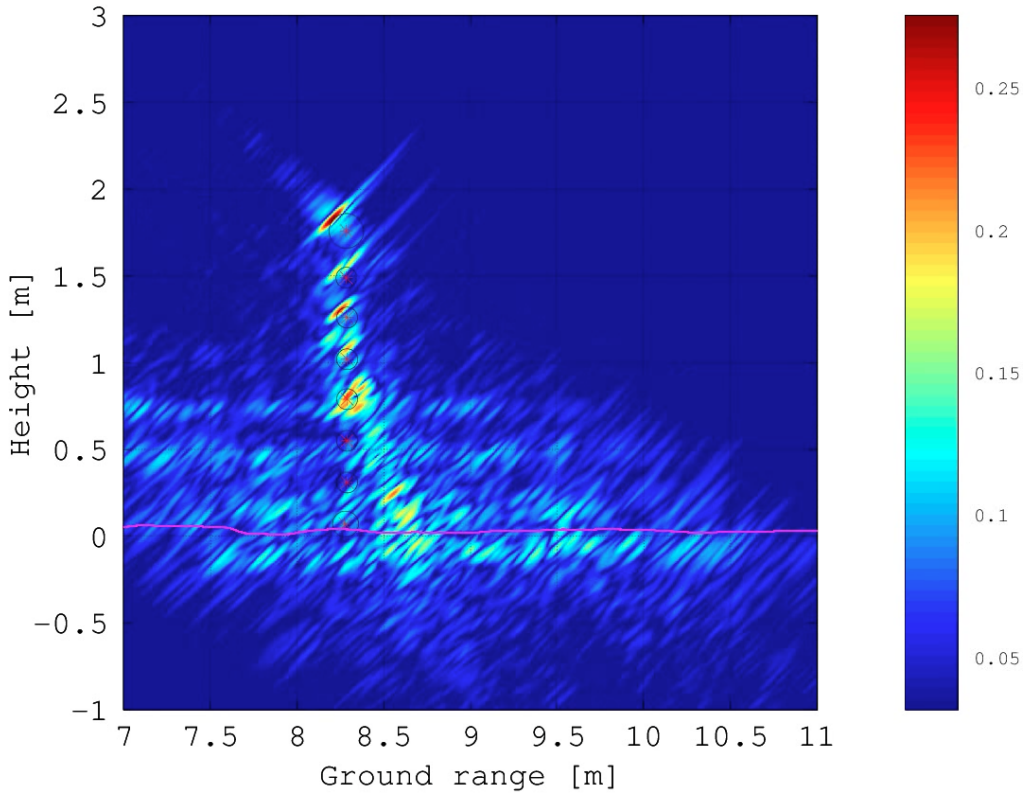
(a) 2016-02-23 (b) 2016-02-23



(c) 2016-02-23 (d) 2016-02-23

Time series of tomographic profiles

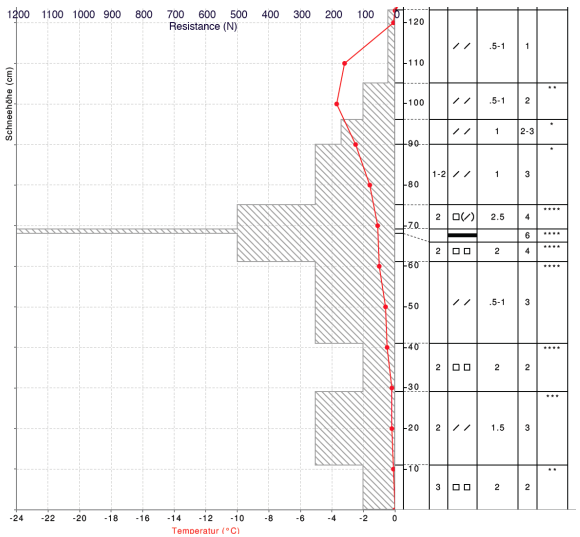
Daily tomograms (since 2015/2016 campaign)!



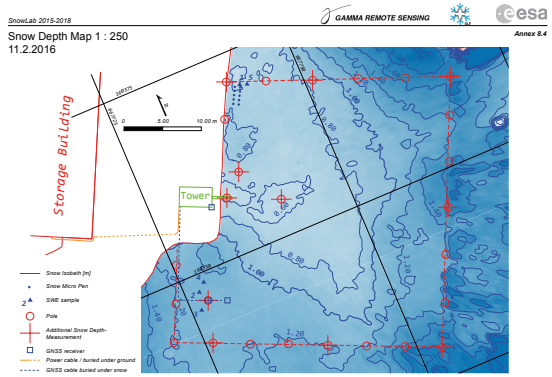
- Time series covers 2015-11-23 until 2016-04-08
- up to 3 tomograms per day, but also gaps due to hardware problems.
- 2016/2017 campaign: 1 tomogram per day.

“In-situ” snow profile, SWE, etc. measurements

Ground truth(?): Quasi in-situ measurements. Highly heterogeneous snow depth in 2015/2016. Much better situation in current 2016/2017 campaign. Site less exposed to strong winds.



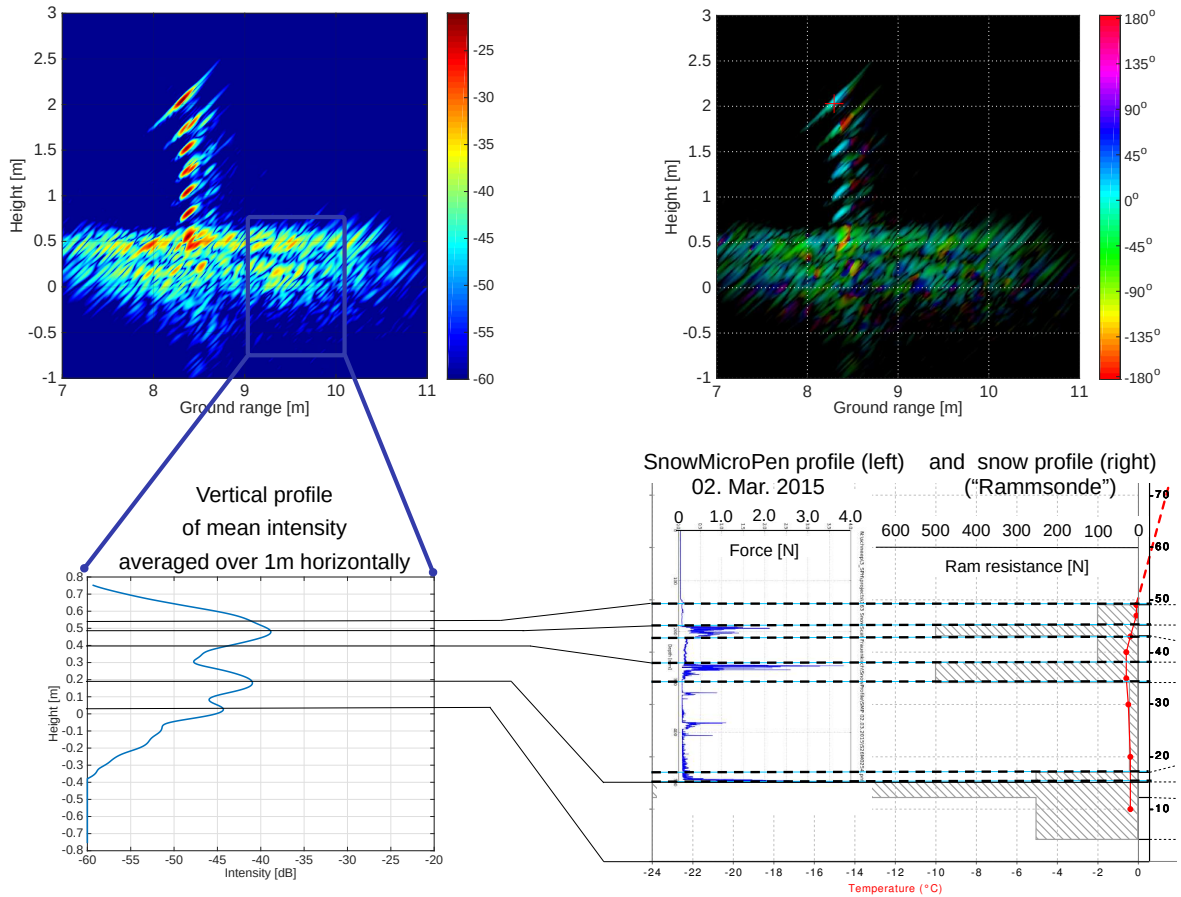




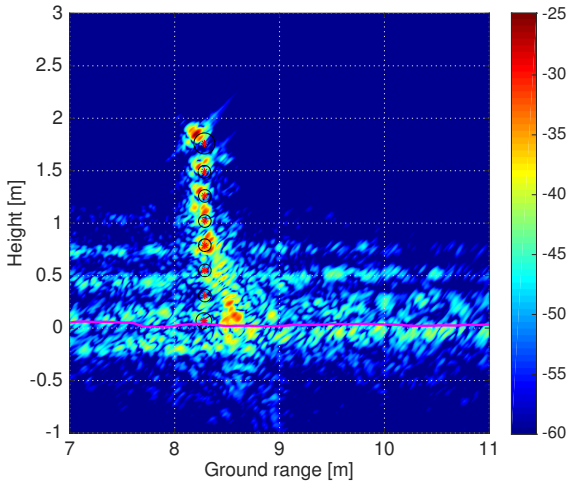


Phase of the complex polarimetric coherence (1)

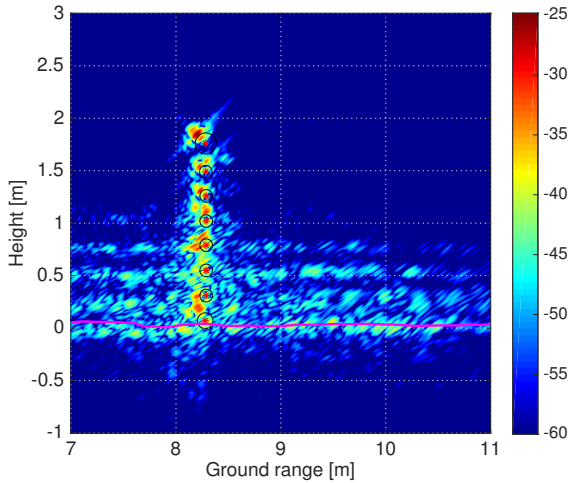
- Co-polar phase between channels HH and VV, combined with HH intensity in a HSV color scheme.
- Hue: phase, saturation: unaltered, set to full saturation. Value: brightness according to intensity in decibel.



Phase of the complex polarimetric coherence (2)



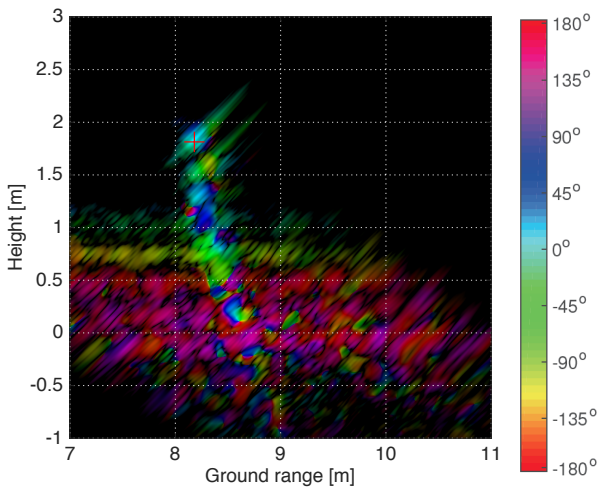
(a) 2016-03-11



(b) 2016-03-11

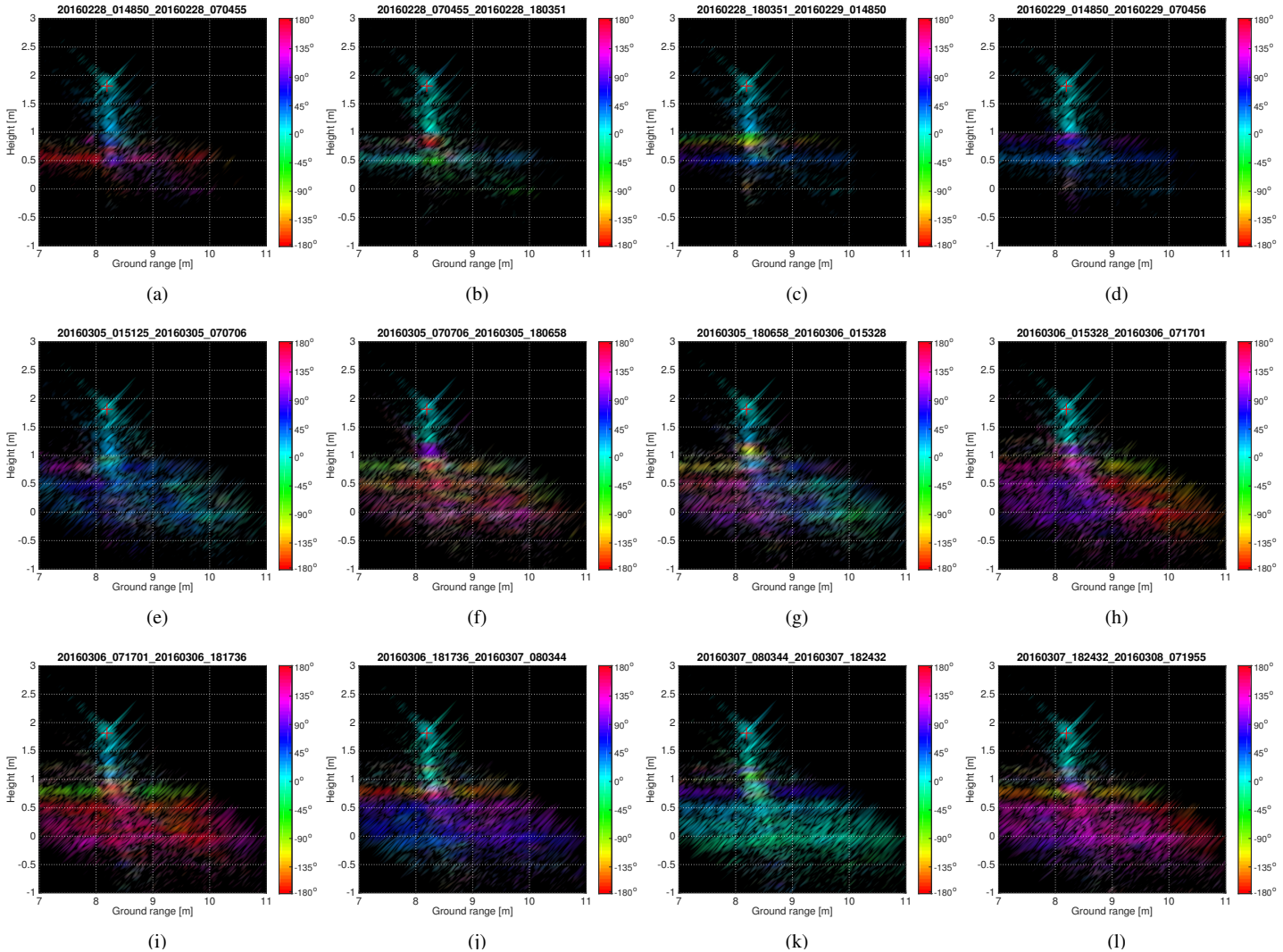


(c) 2016-03-11

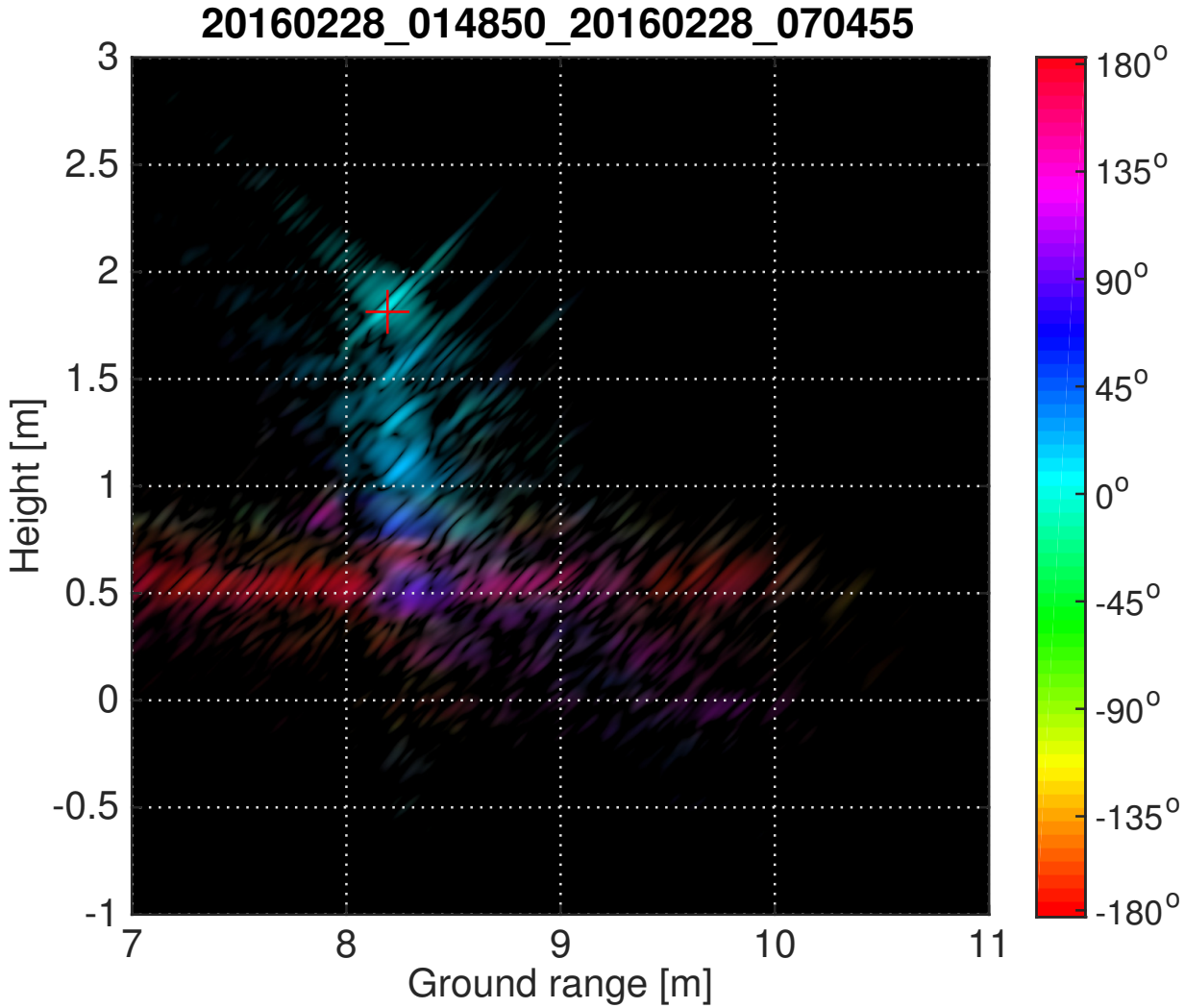


(d) 2016-03-11

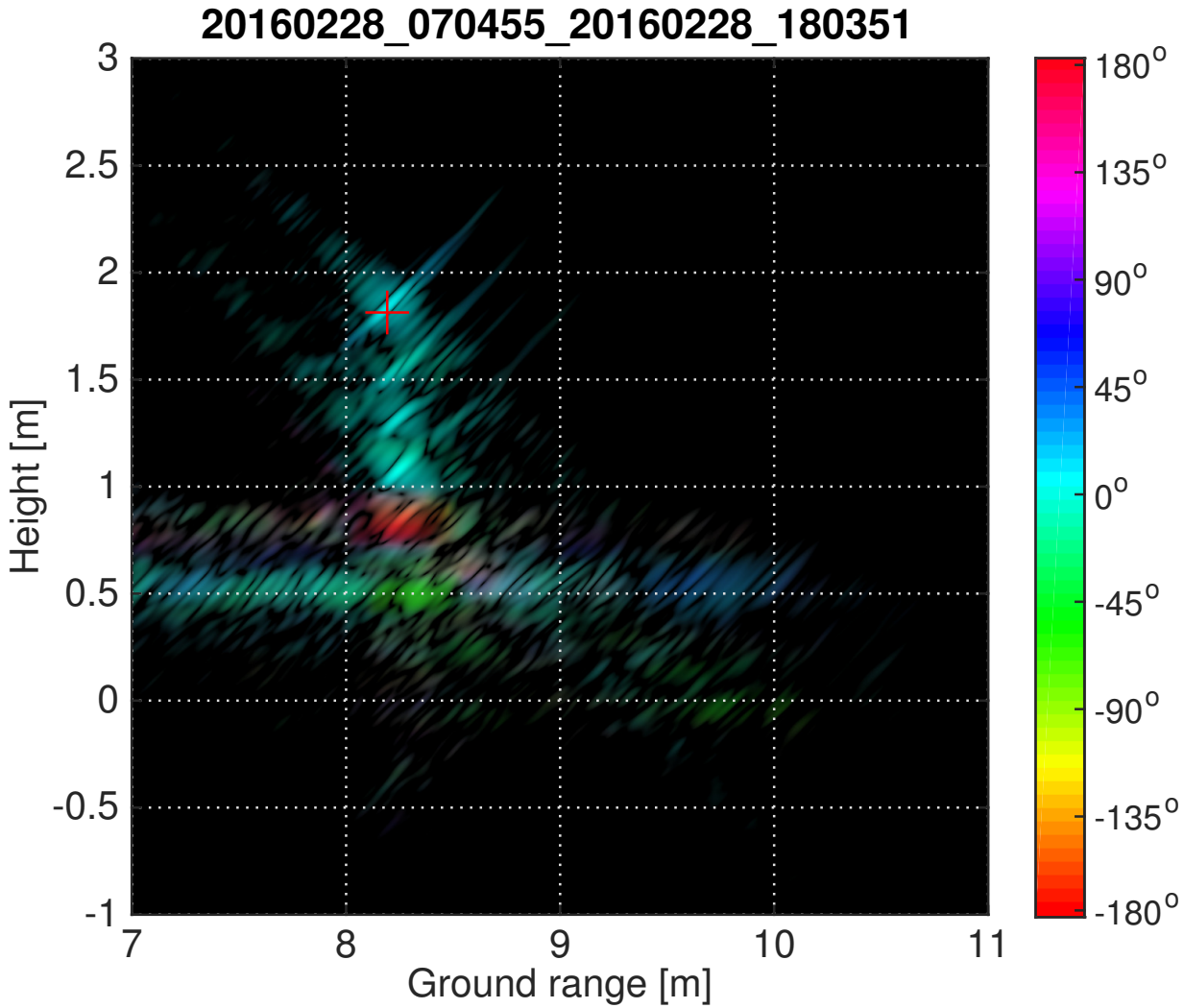
Temporal interferograms of tomographic profiles



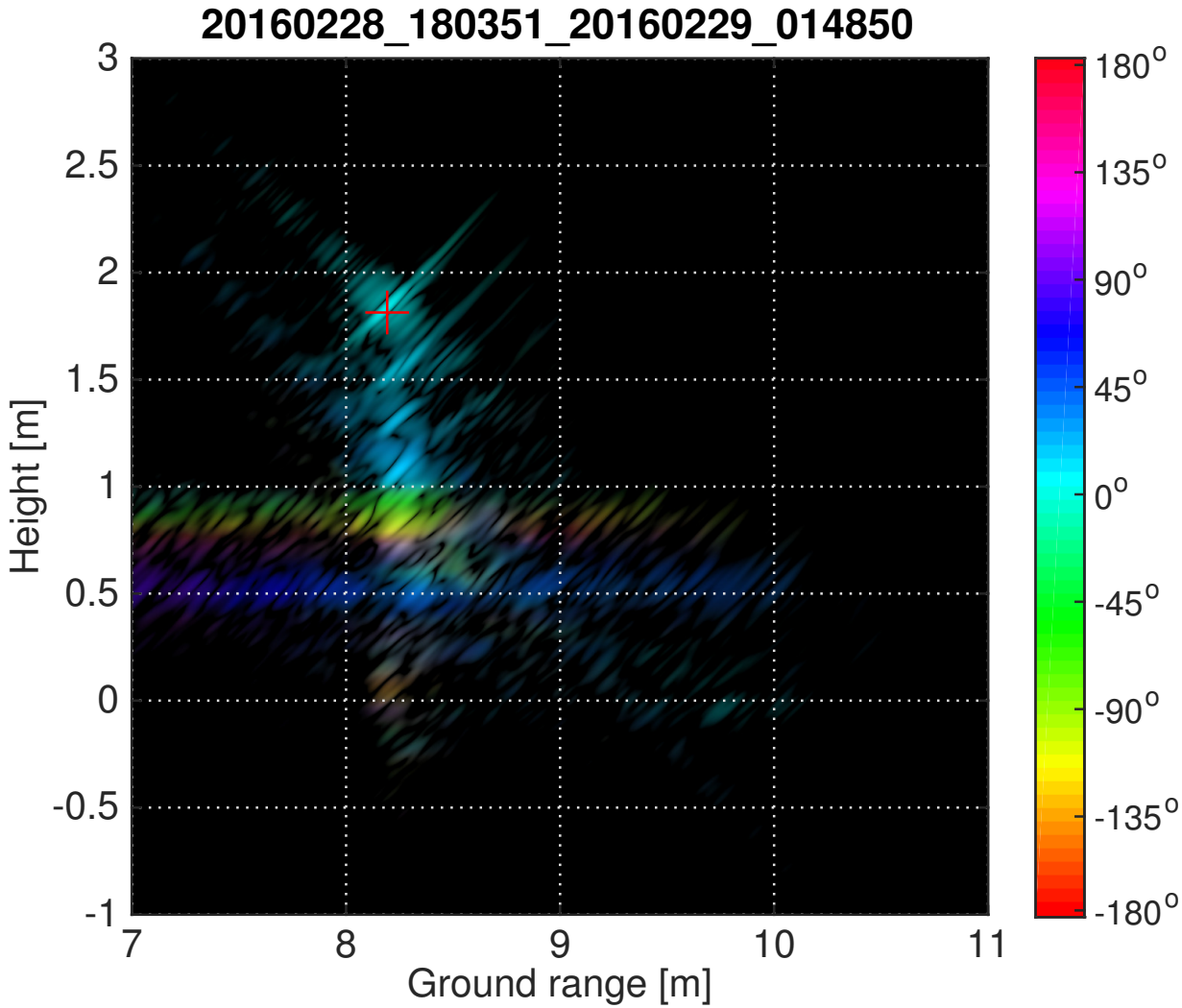
Temporal interferograms of tomographic profiles



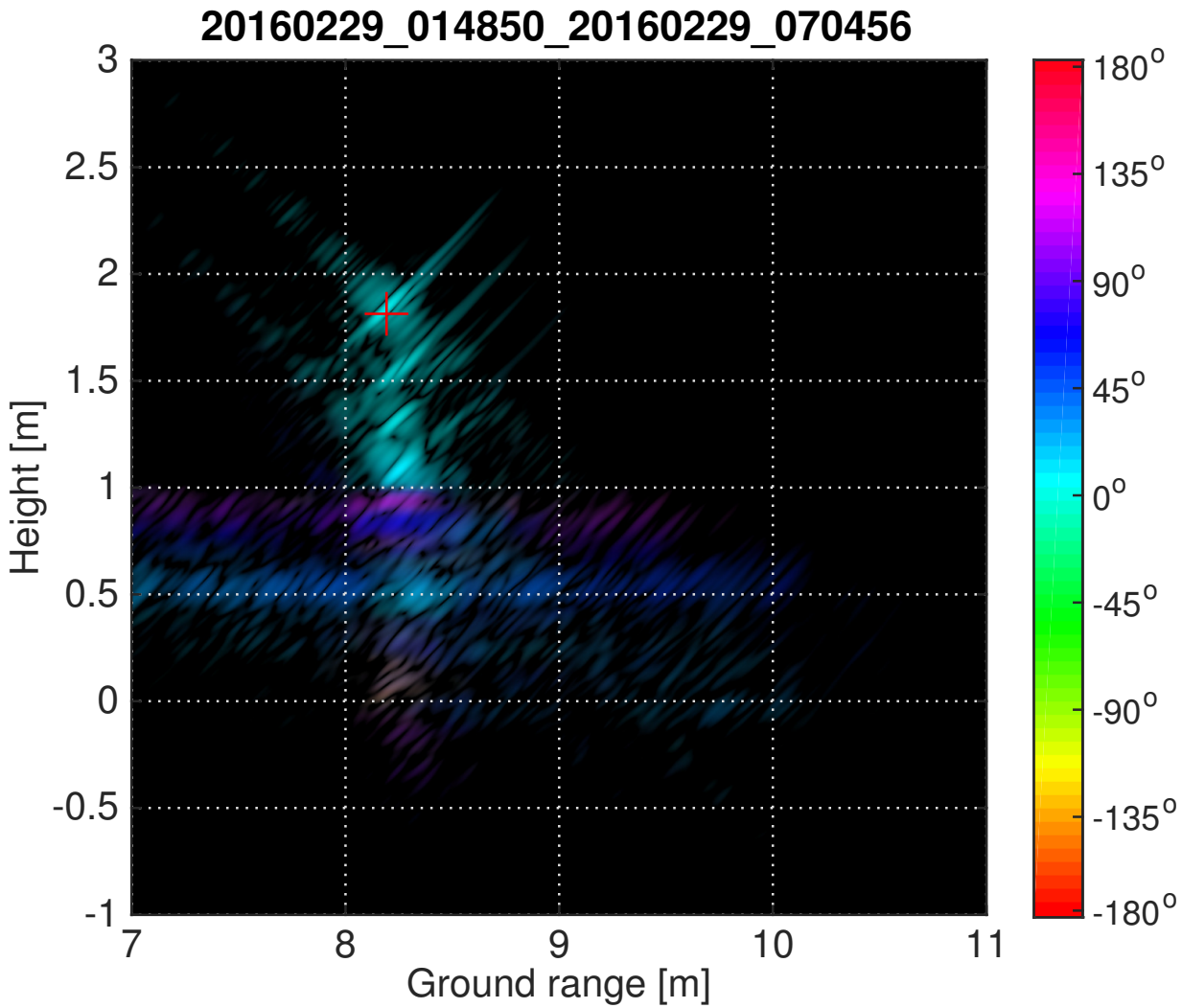
Temporal interferograms of tomographic profiles



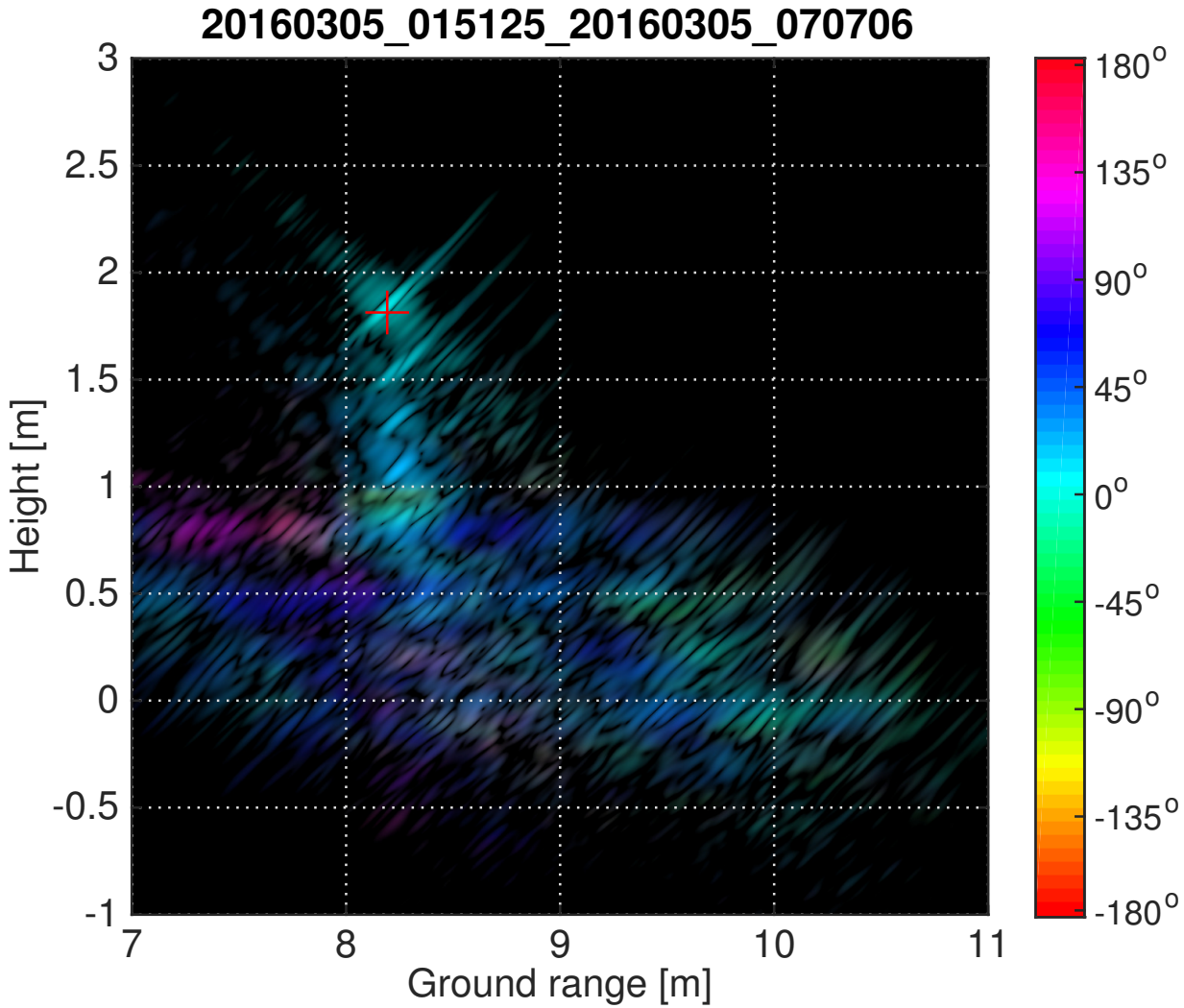
Temporal interferograms of tomographic profiles



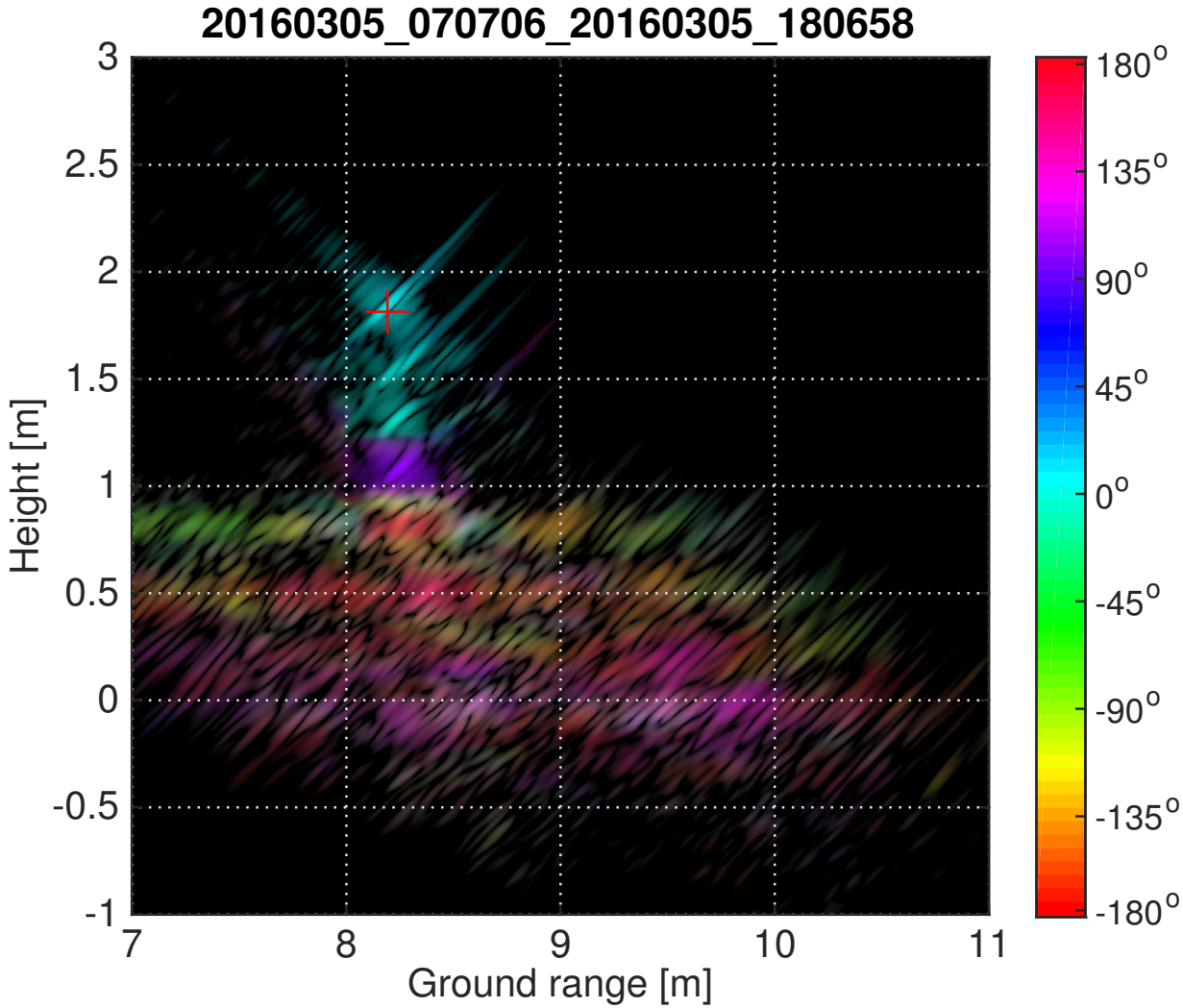
Temporal interferograms of tomographic profiles



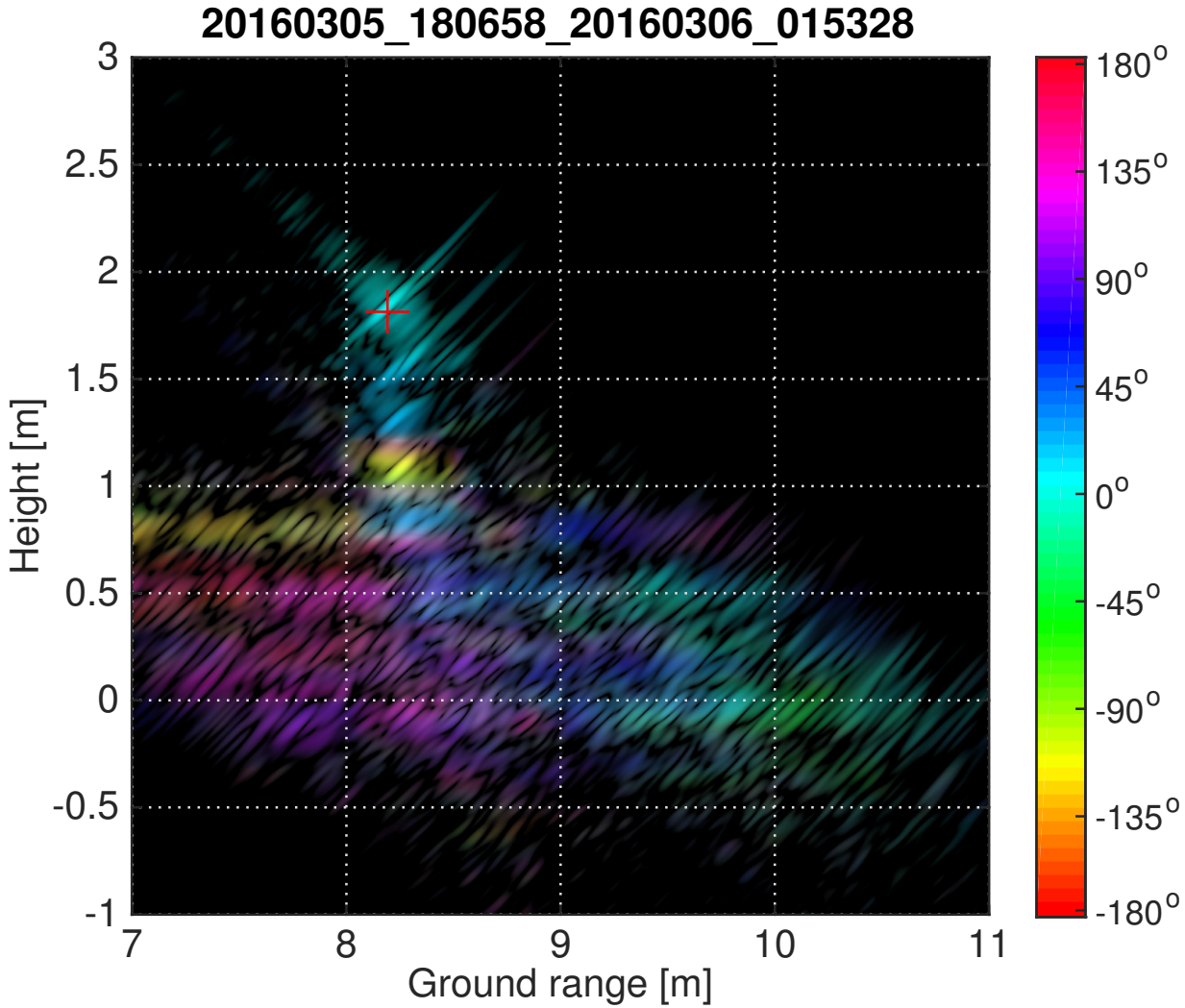
Temporal interferograms of tomographic profiles



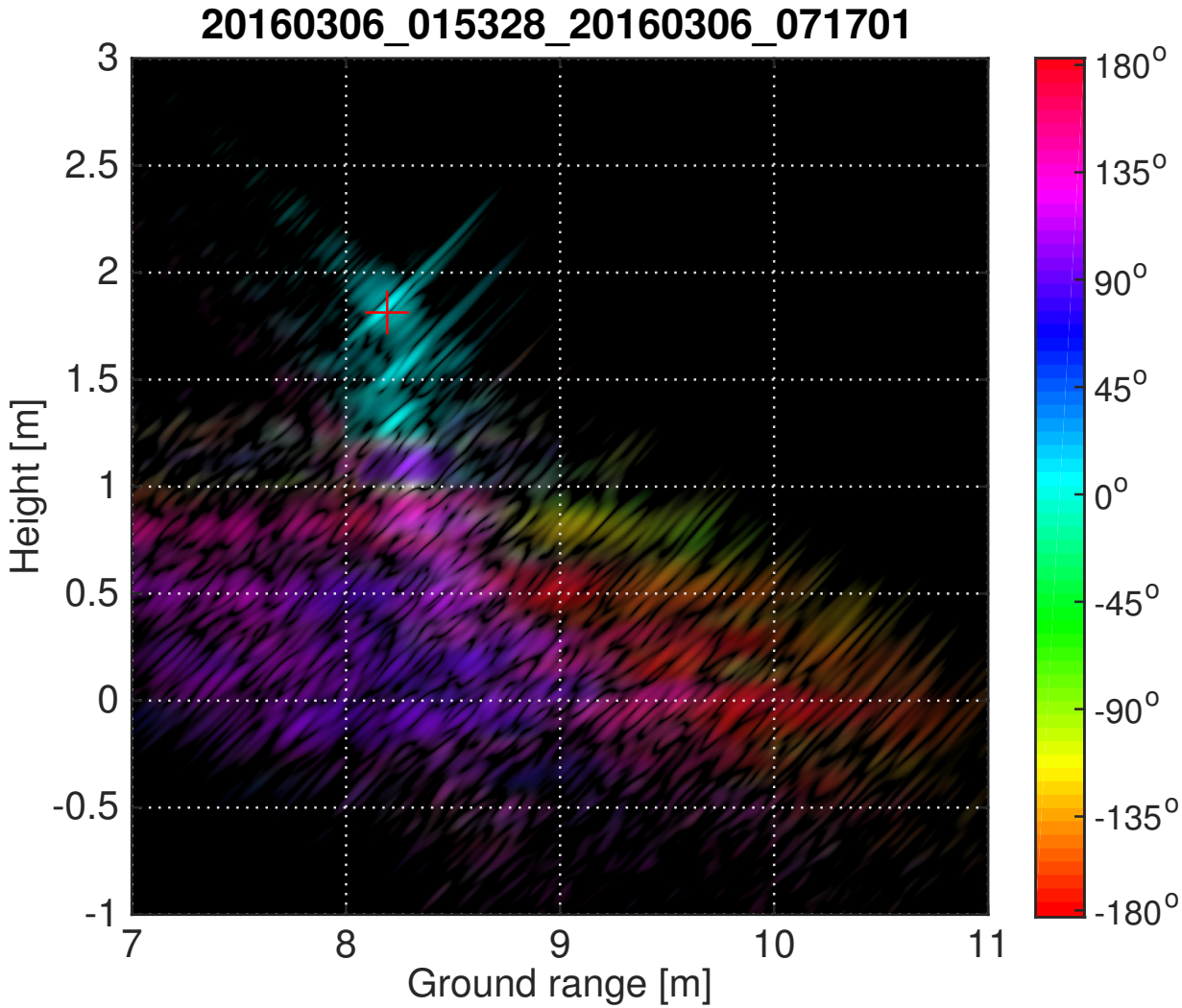
Temporal interferograms of tomographic profiles



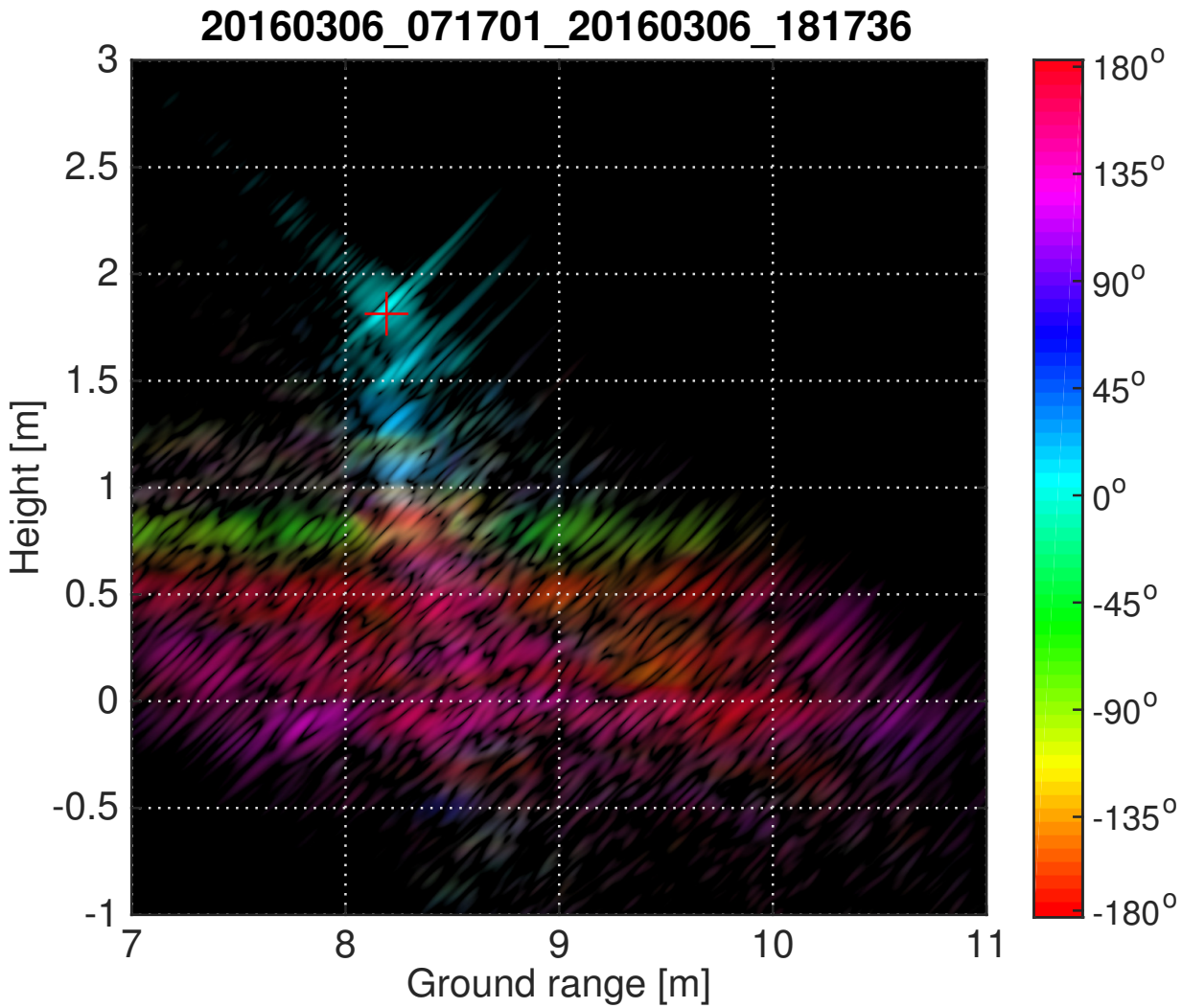
Temporal interferograms of tomographic profiles



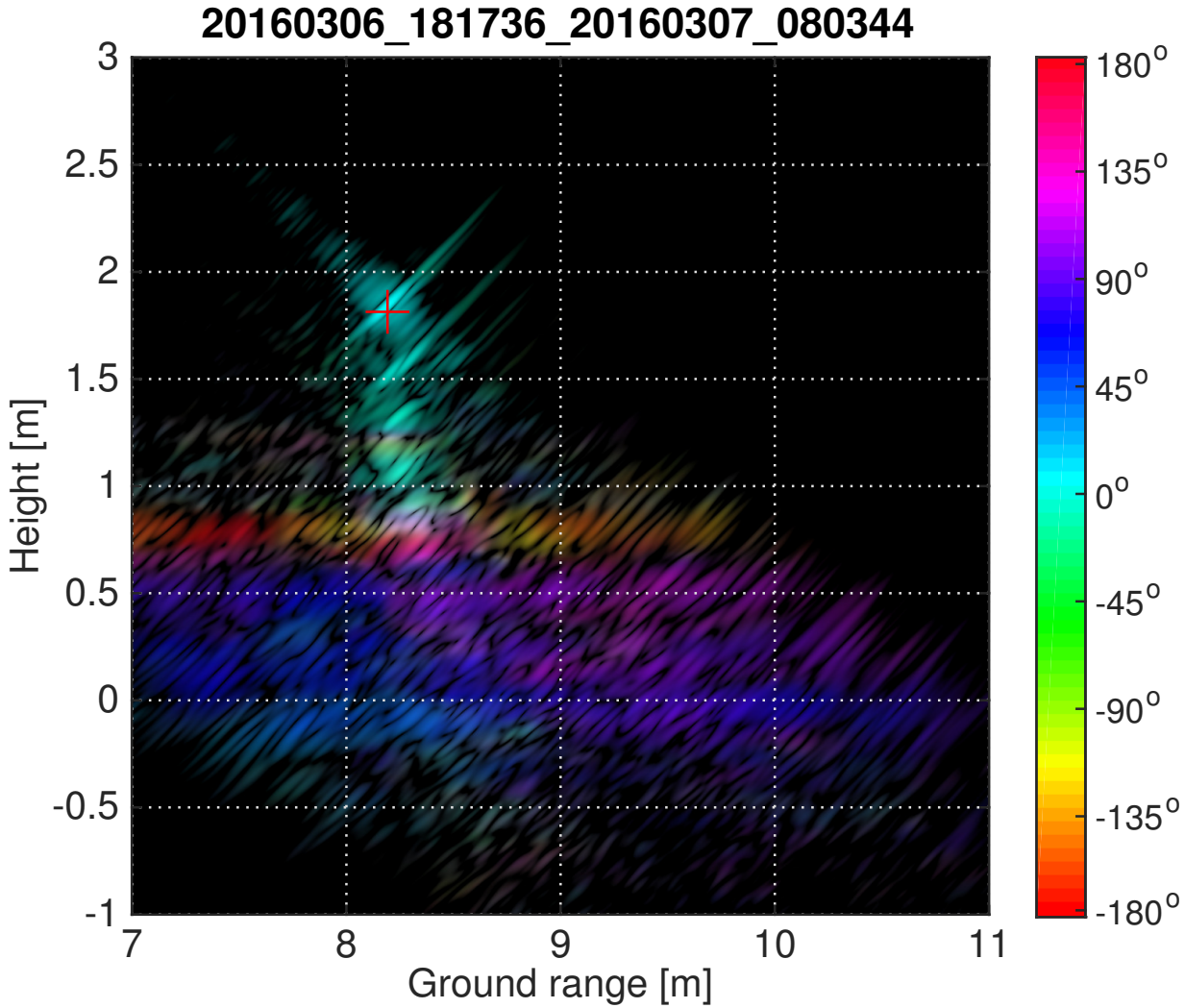
Temporal interferograms of tomographic profiles



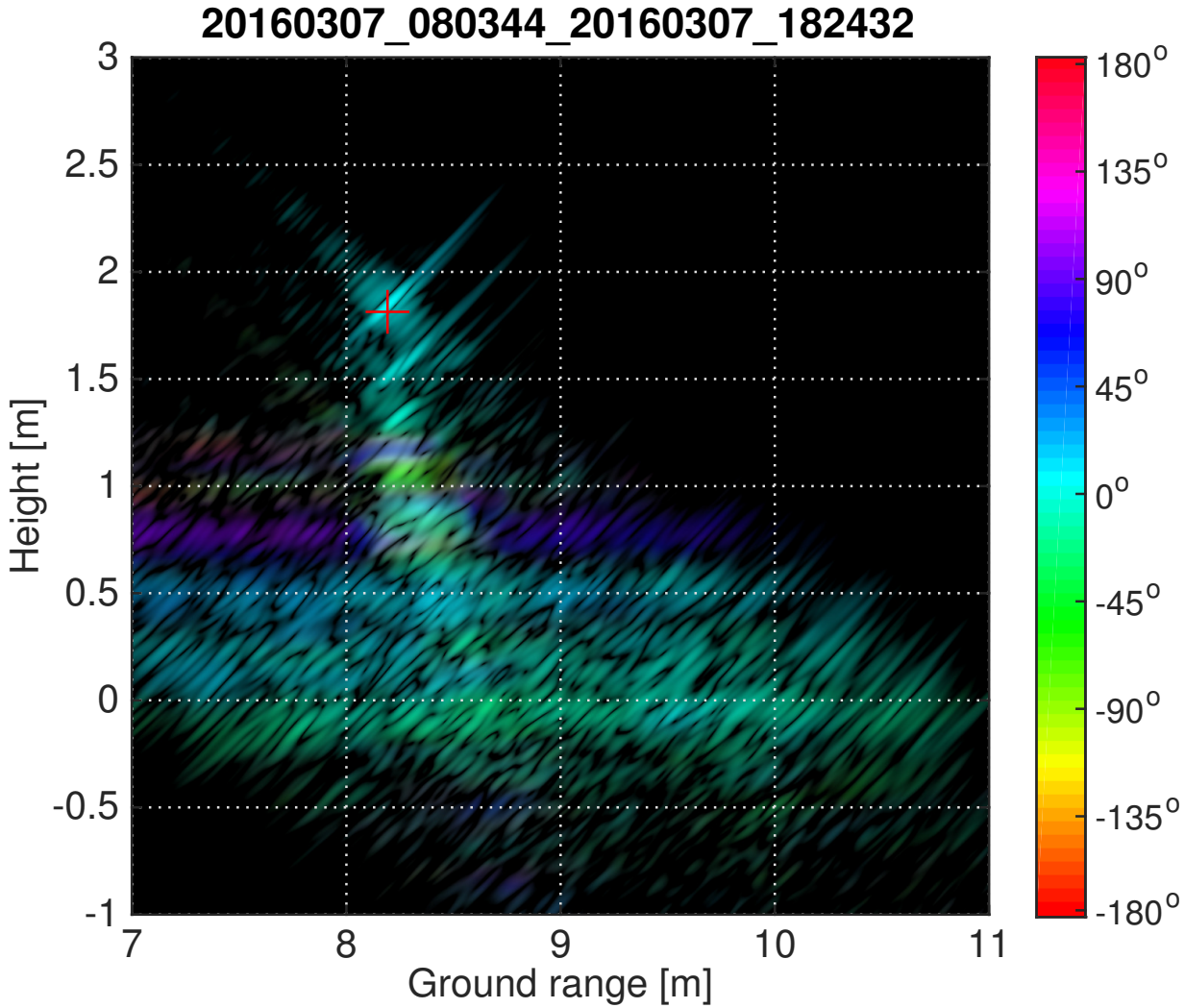
Temporal interferograms of tomographic profiles



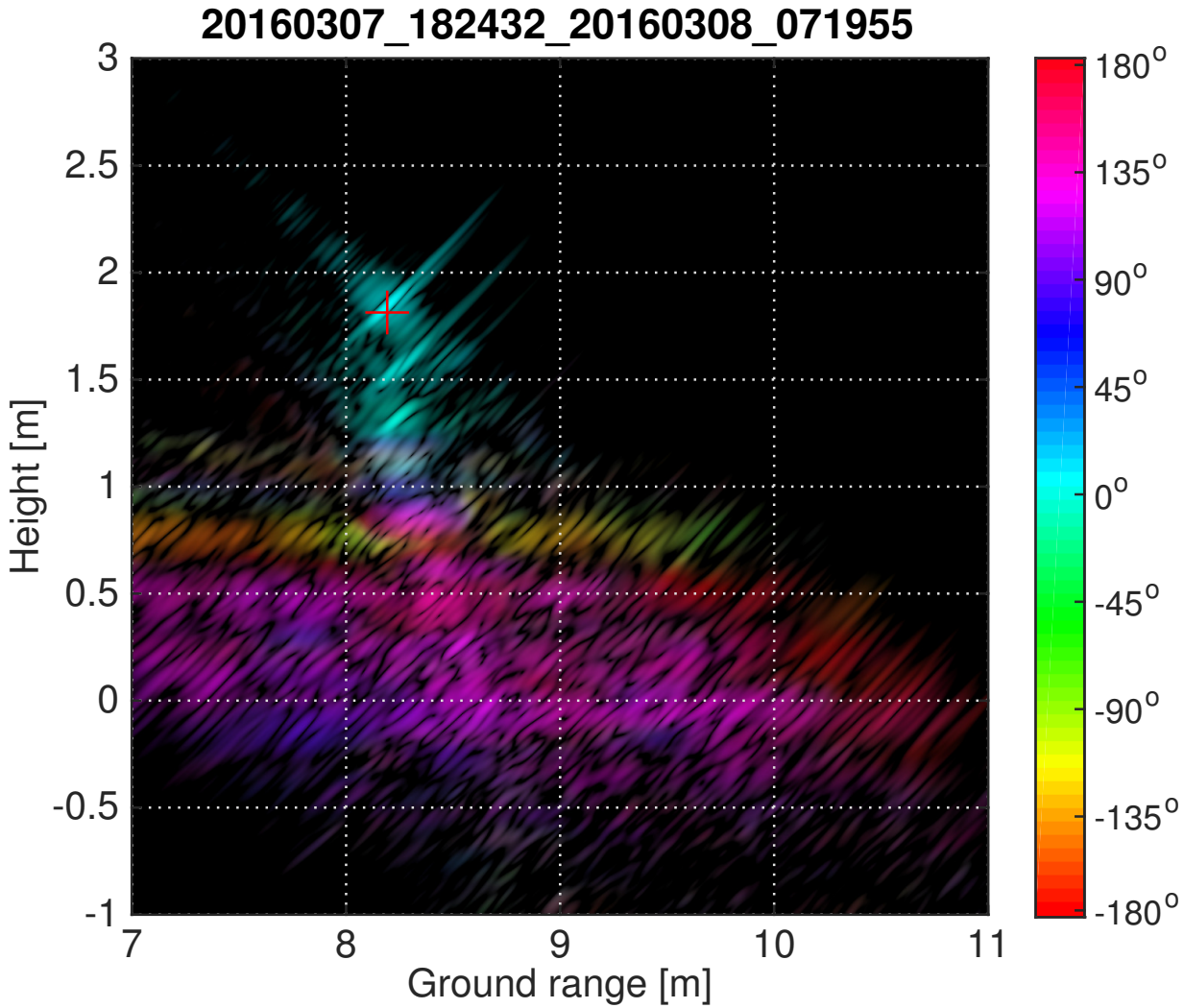
Temporal interferograms of tomographic profiles



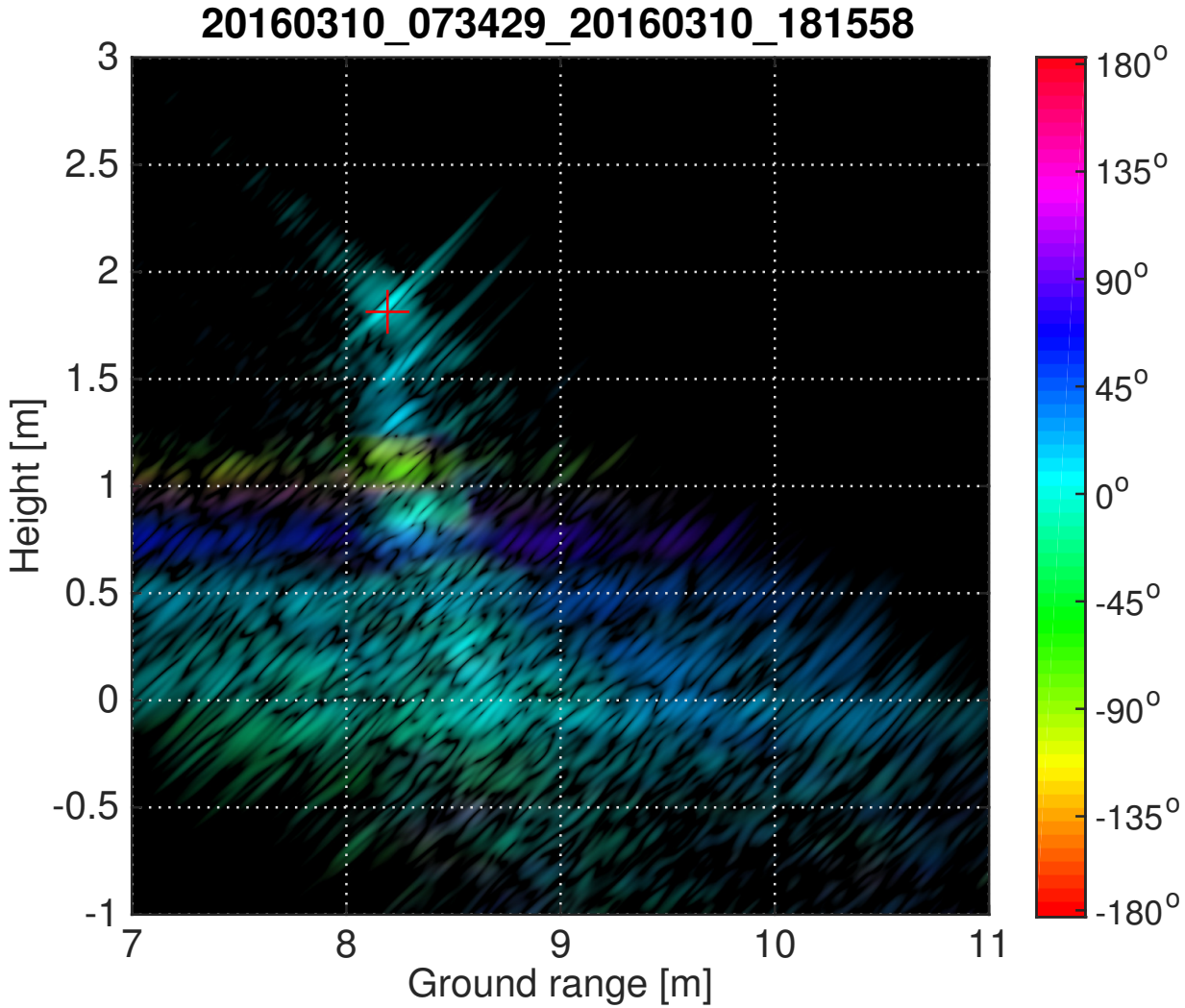
Temporal interferograms of tomographic profiles



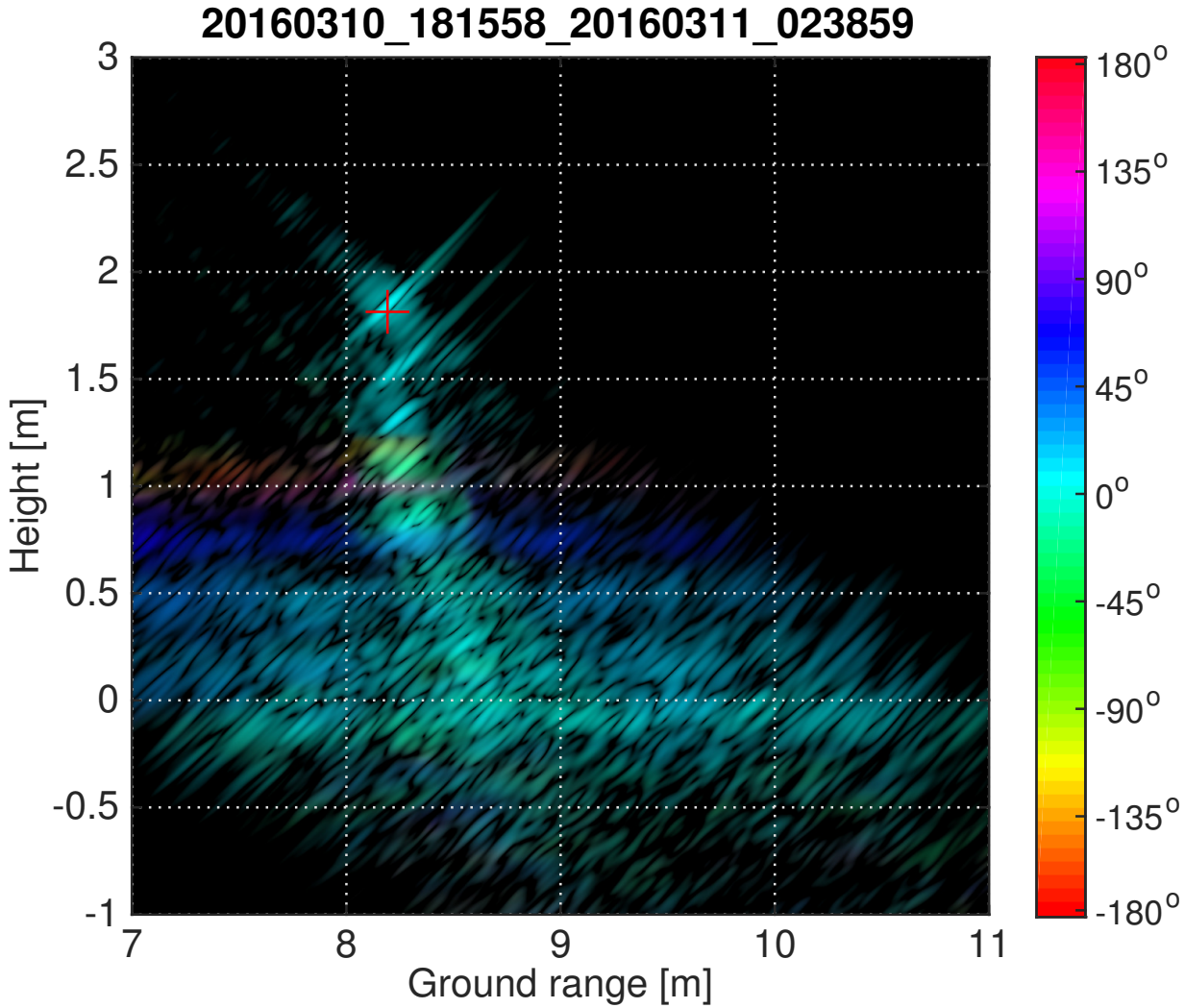
Temporal interferograms of tomographic profiles



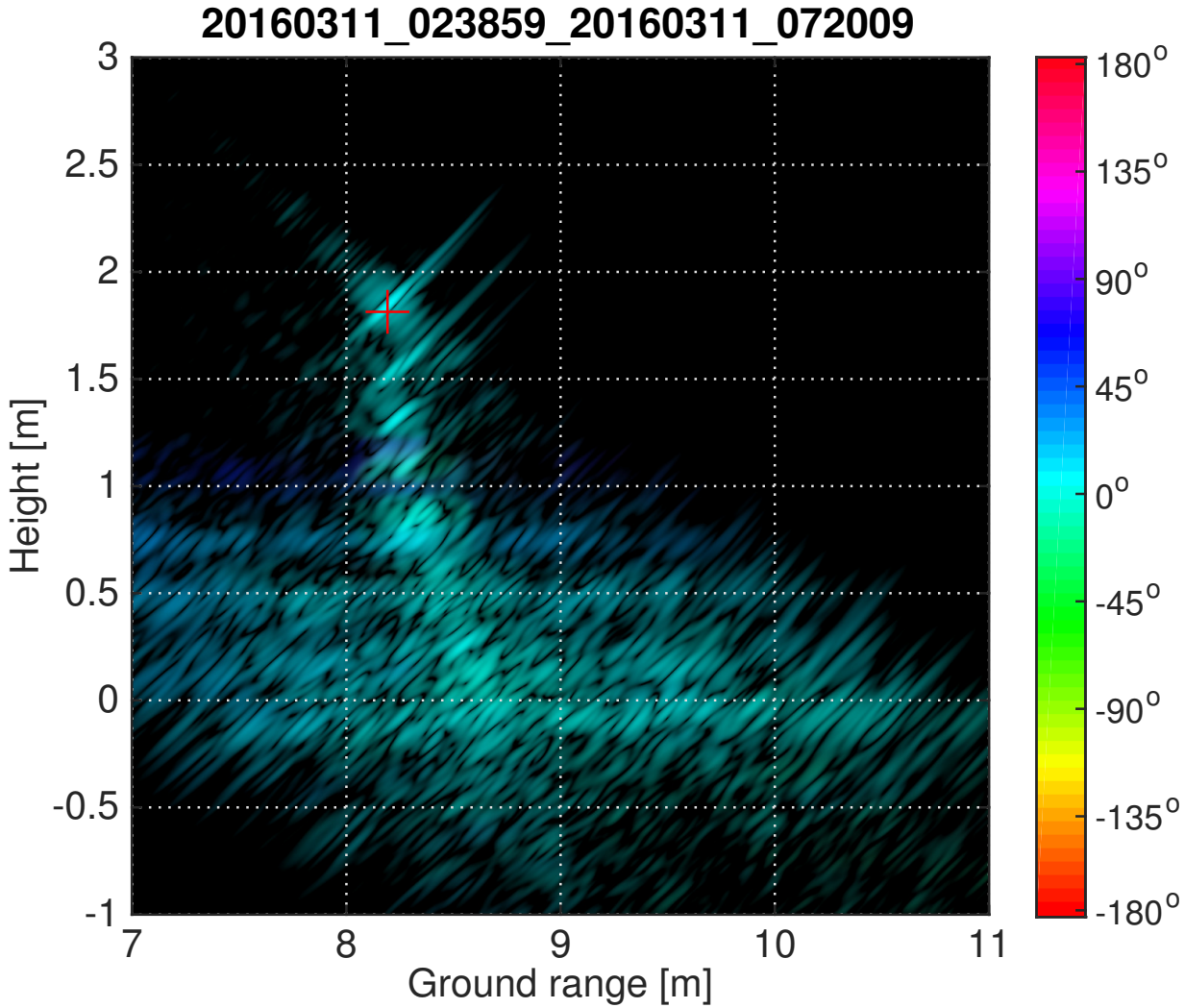
Temporal interferograms of tomographic profiles



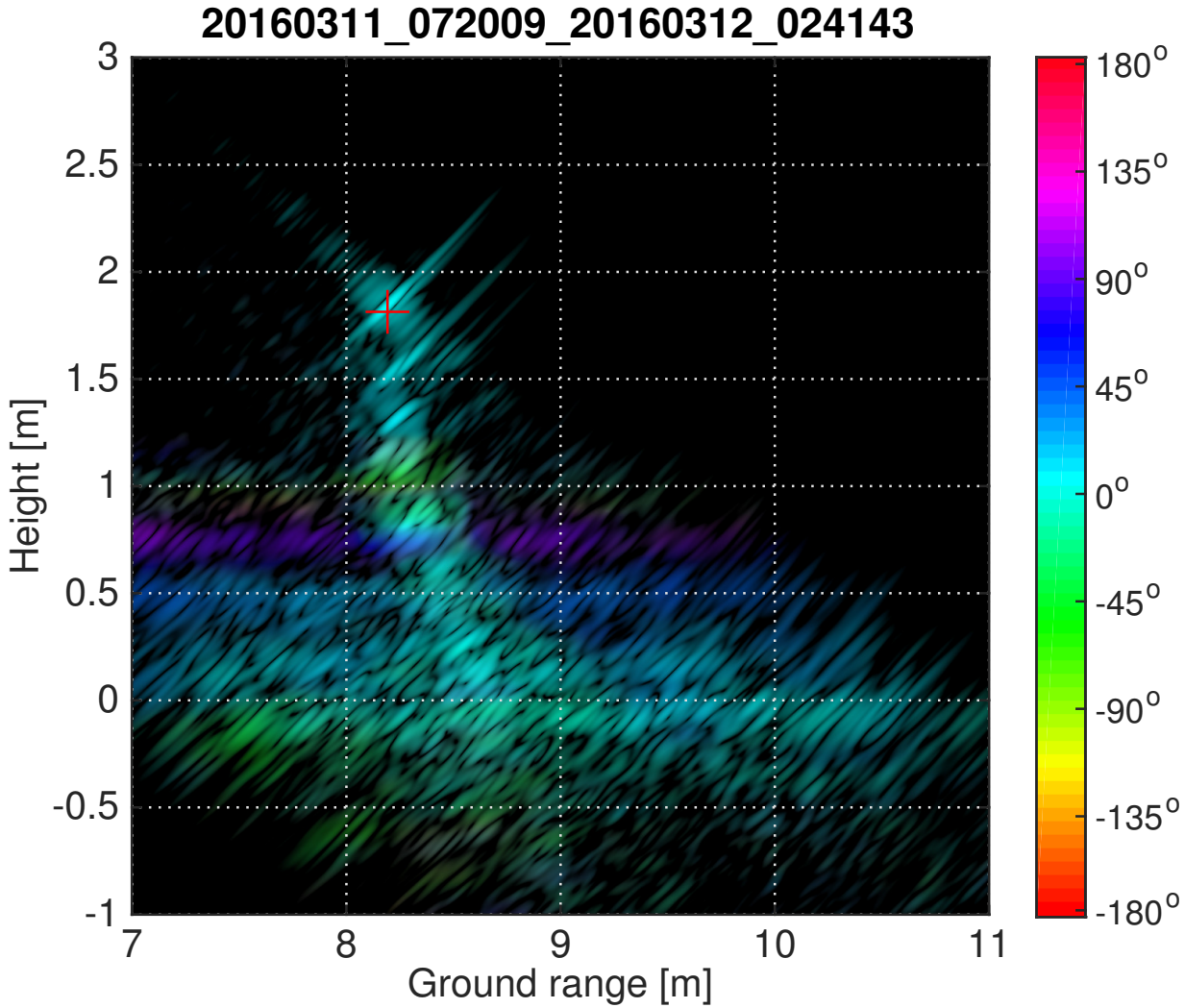
Temporal interferograms of tomographic profiles



Temporal interferograms of tomographic profiles



Temporal interferograms of tomographic profiles



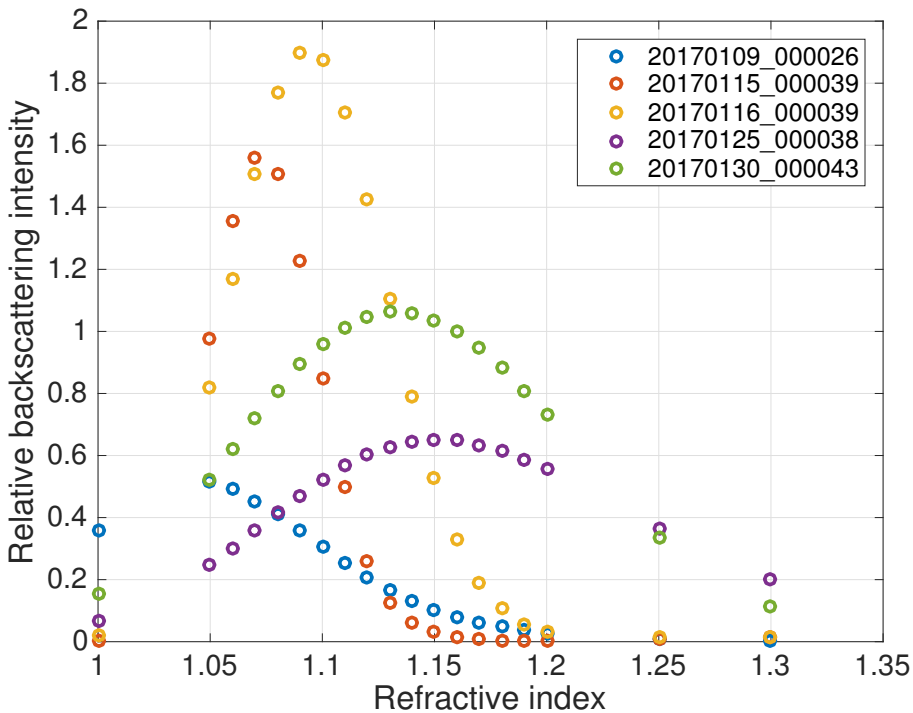
Further development of tomographic processing/analysis tool for the ESA SnowScat

Extraction of refractive index by searching for max. relative intensity

- Approach towards an automated extraction of the refractive indices:
- Based on the spheres of the tomographic test target.
- Idea: refraction affects the focused image mainly through displaced appearance (and the focusing quality (sharpness))
- Estimate the refractive index through maximum search using the image intensity I as the merit function at specific target regions

Extraction of refractive index by intensity maximization (2)

$$\hat{n}_s = \underset{n_s \in \mathbb{N}_s}{\arg\max} \left(\hat{I}(n_s) \right)$$



Extraction of refractive index by intensity maximization (3)

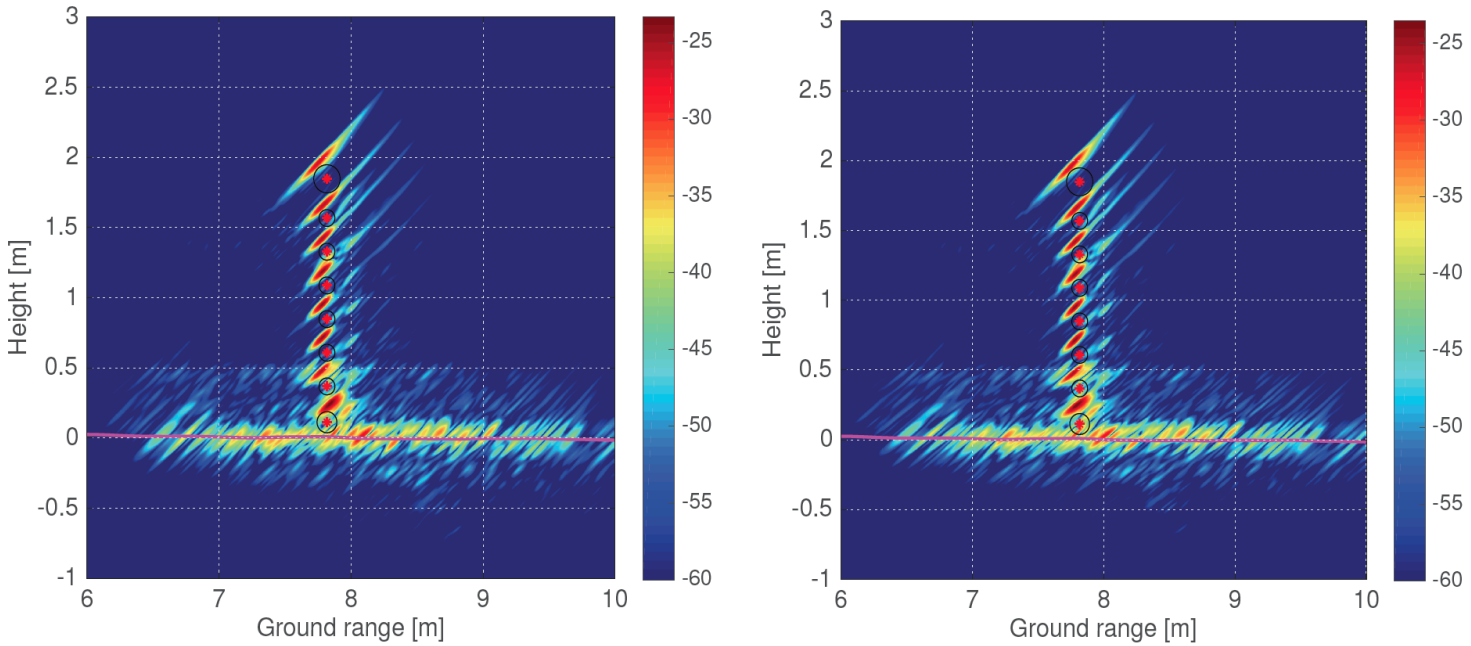
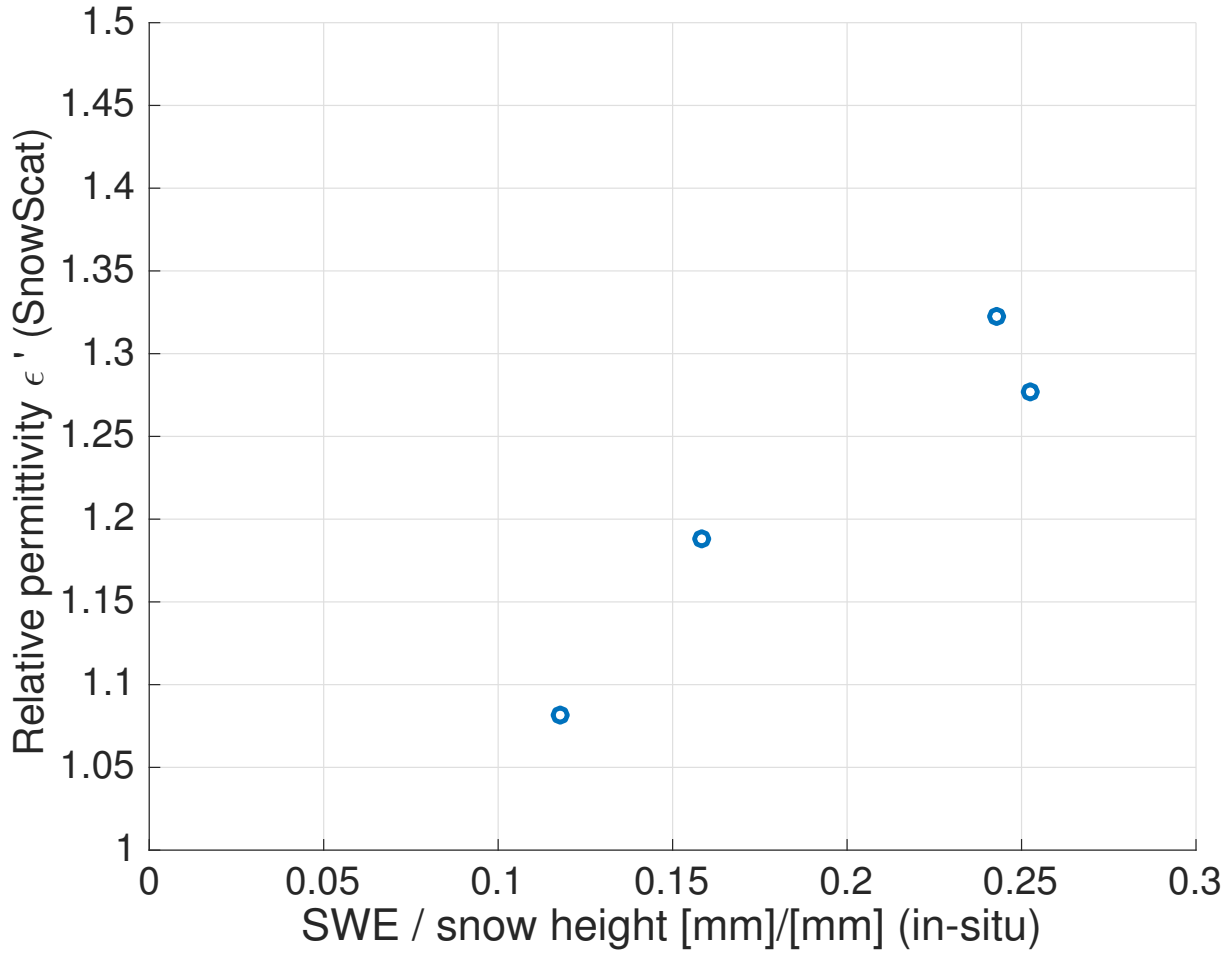
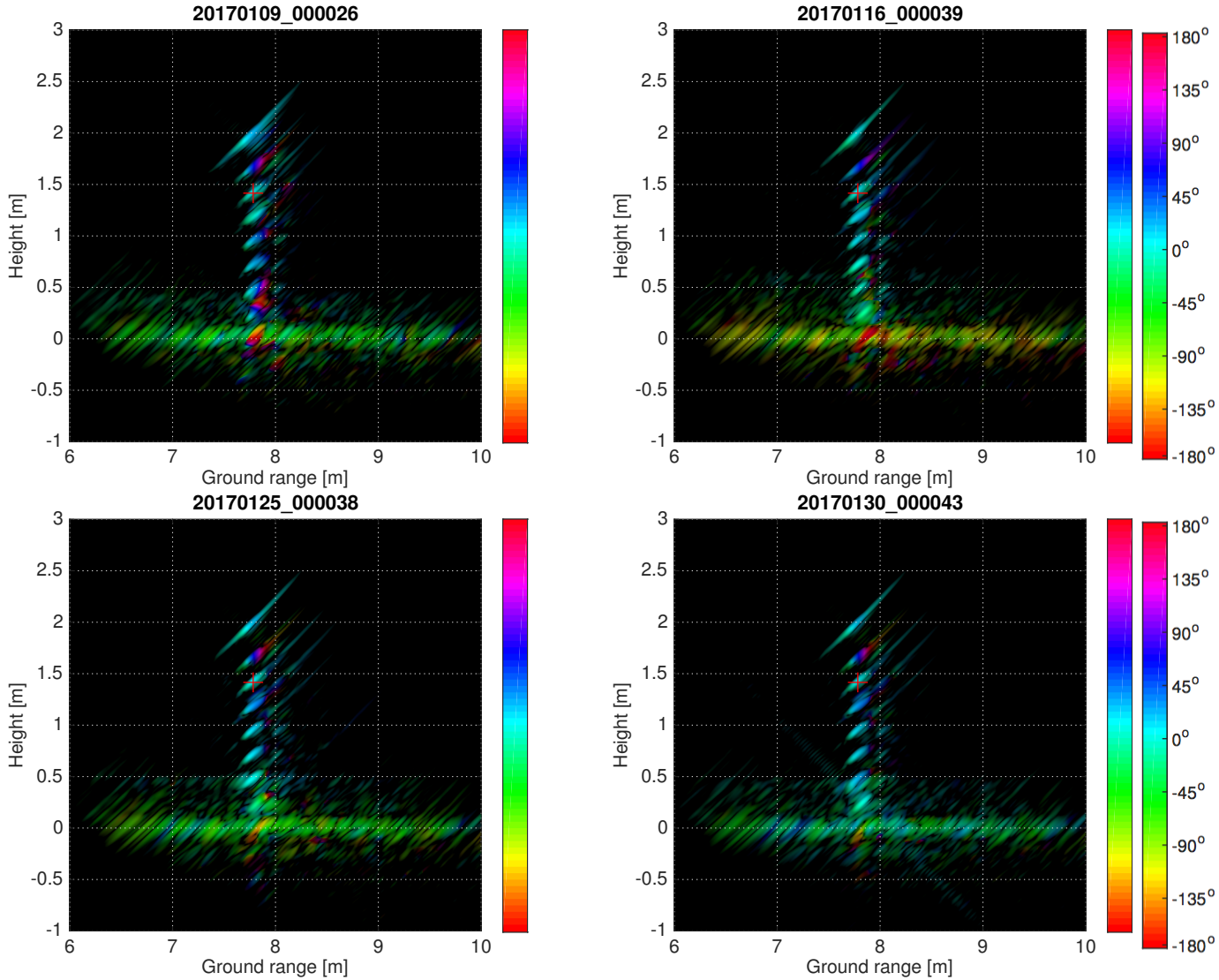


Figure 2: Focused tomographic profile without (left) and with (right) taking into account the estimated refractive index for the snow pack as obtained from the maximization.

First comparison: extracted rel. permittivity vs. in-situ SWE / snow height



Examples co-polar phase differences 2016/2017



Conclusion/Outlook

- Second (more) comprehensive SnowScat tomographic campaign (ongoing) within ESA SnowLab project (+ 2017/2018 upcoming).
  - 2015/2016 lots of snow, complicated structure, limited in-situ measurements.
  - 2016/2017 less snow (lower altitude) but much better “initial conditions and more frequent and more elaborate in-situ data.
- (Ongoing) Refinement of the tomographic processing tool (automated extraction of refractive indices e.g. using DInSAR phase on top of first order correction of refraction.)
- Quantitative assessment of 2016/2017 time series of tomographic profiles versus new in-situ data and derived snow parameters by SLF:
  - refractive indices, through refocusing and DInSAR vs. SWE,
  - anisotropy (copolar phase difference vs. microCT),
  - relative backscattering contribution of different layers (crusts) within snowpack, vs. snow micro pen.

Acknowledgment

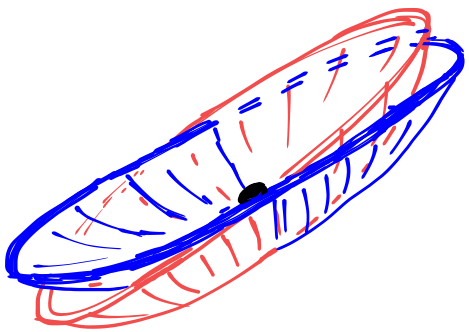
Funding through ESA/ESTEC projects

- “Enhancement of SnowScat for tomographic and vertical profiling observation capabilities” and
- ESA SnowLab project (ongoing).

A. Henzen at KWO hydroelectric power company, Innertkirchen, Switzerland for supporting the in-situ measurements in 2015/2016.
M. Jaggi at SLF, Davos, for the in-situ snow characterisation.

Additional slides

Limitations



Wavefronts impinging at any scatterer location from 2 different elevation angles.

In terms of hardware/system:

- In elevation: high resolution through beamforming.
- BUT, in azimuth: limited resolution governed by beamwidth.
- Has implications on aperture synthesis in elevation as signal contributions that “do not belong” to the same target are coherently summed.
  $\Rightarrow$ Lower signal to clutter ratio.
- Synthetic aperture in azimuth would be preferable.
  $\Rightarrow$ Trade-off: performance / resolution vs. size / weight / portability / cost.
- Long acquisition time for tomo profile with full-pol + 5 pointing directions.

Lessons learned:

- (Semi-)controlled “field lab” conditions:
- Strong spatial variability of snow pack due to harsh weather/wind conditions in Alpine environment.
- Somewhat limiting regarding in-situ measurements/validation.

SnowScat's max. resolution in elevation direction

Stripmap-mode resolution

$$\delta_n = \frac{\lambda_c r_0}{2L} (= 0.05m),$$

max. synth. apert. L=2.22m.

Range @ PCA: r_0 = 9 m,

for unconstrained beamwidth.

BUT, $\theta_{bw} = \lambda/D$ of SnowScat:

[9.0^o, 4.6^o].

So, for r_0 = 9 m $\rightarrow$ $L_{st} = 0.72m$

based on $\theta_{bw} = 4.6^o$

$\Rightarrow$ Max. resolution in elevation:

$$\delta_{n_{st}} = \frac{\lambda_c r_0}{2L_{st}} = 0.15m$$

Spotlight-mode resolution

$$\delta_{n_{sp}} \approx \frac{\lambda_c}{4\sin(\phi_0)}$$

λ_c : central wavelength.

ϕ_0 : half-angle of integration.

Extreme case: semi-circular aperture

($\phi_0 = 90^o$):

$\delta_{n_{circ}} = \lambda_c/4$.

SnowScat setup: $\phi_0 = 7^o$

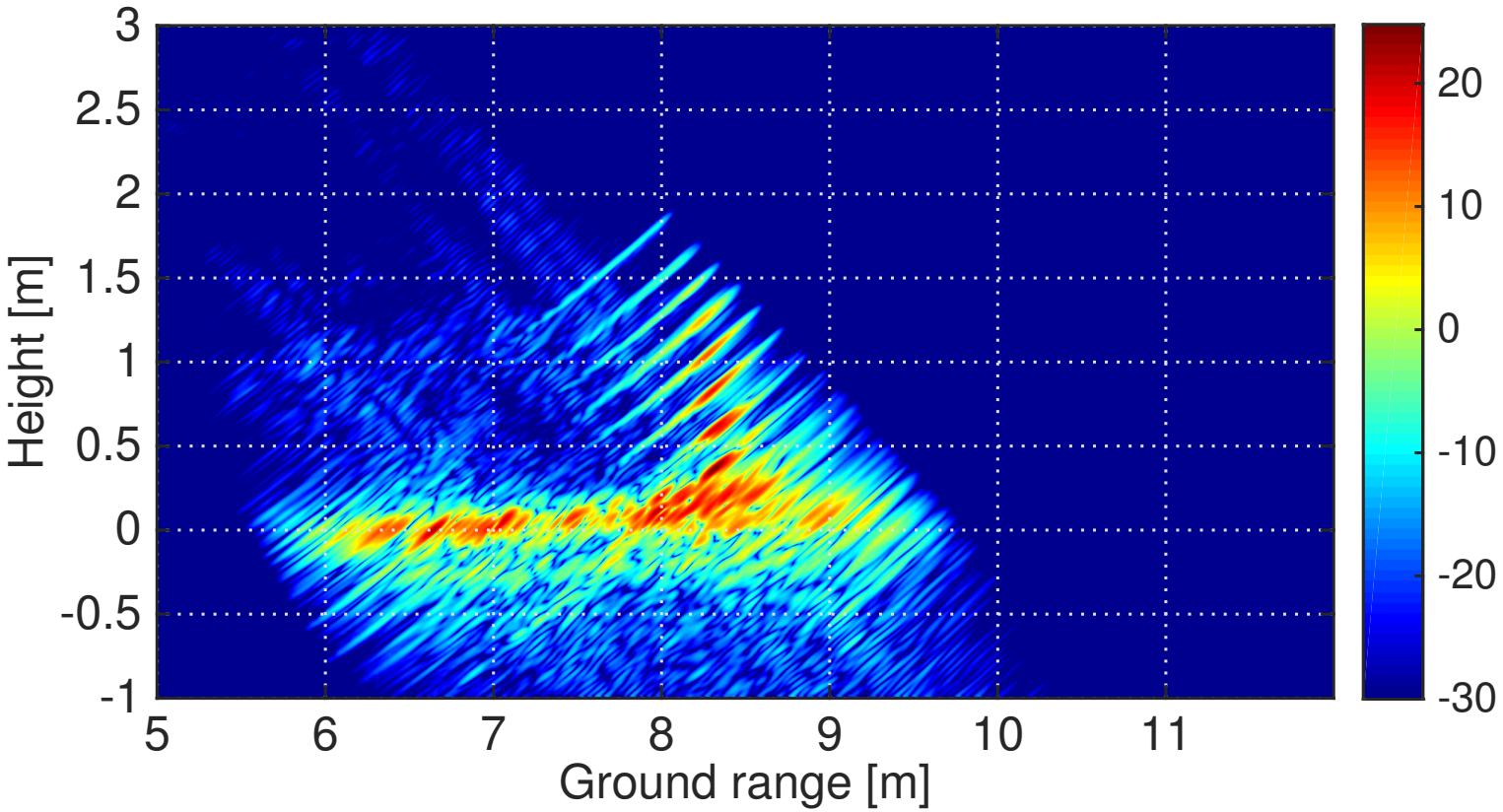
$\Rightarrow$ Max. resolution in elevation:

$$\delta_{n_{sp}} = \frac{\lambda_c}{4\sin(\phi_0)} \approx 0.05m$$

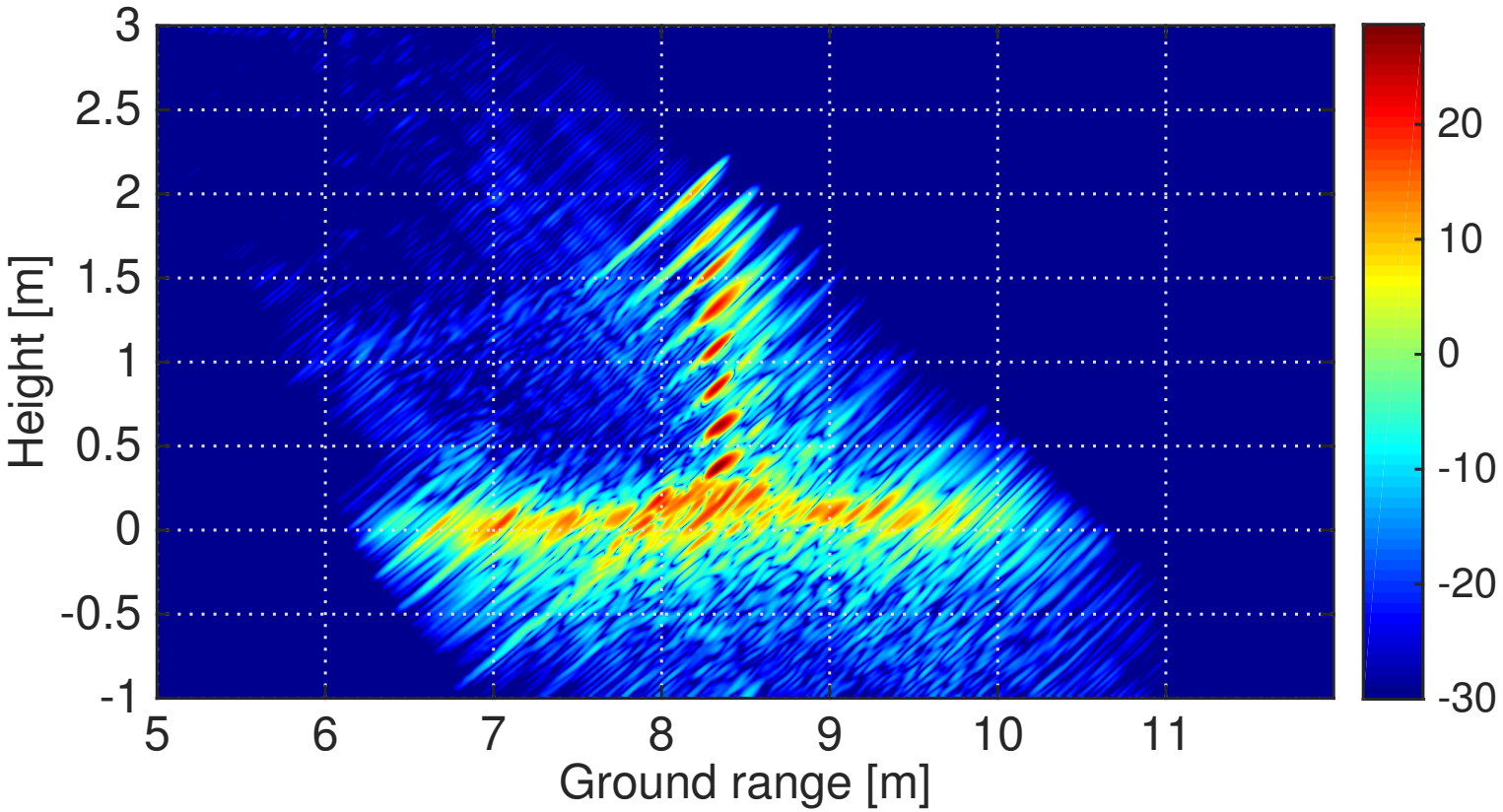
Tomographic focusing using data taken at different elevation angles

- Beamwidth of the SnowScat device is too narrow to cover the entire range of elevation angles needed for tomographic profiling of the tomographic test target.
- Individual tomograms at 5 different elevation angles (39^o, 42^o, 45^o, 48^o, 51^o) were processed separately.
- Coherent addition of individual tomograms.

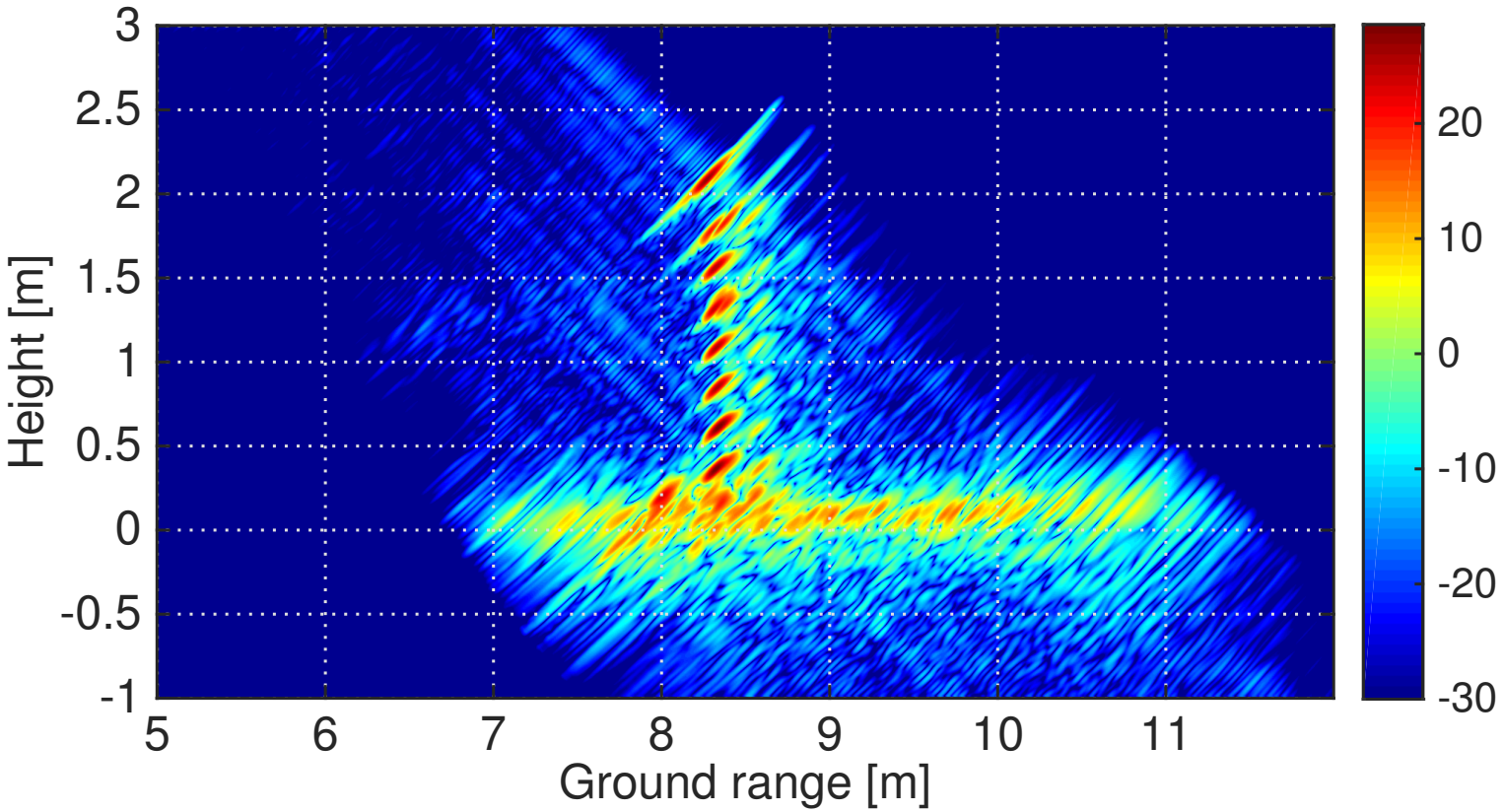
Tomographic focusing at elev. 39^o



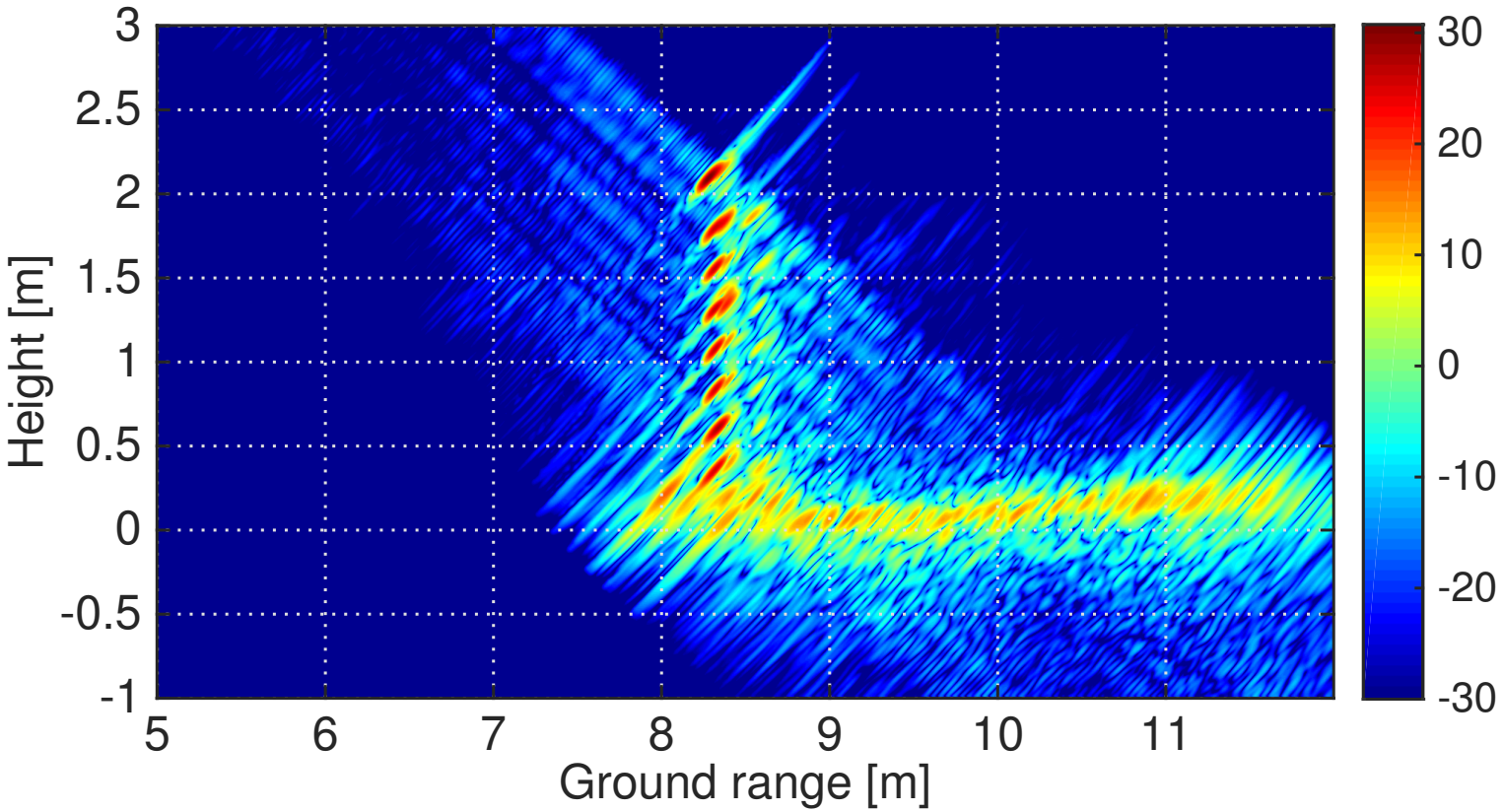
Tomographic focusing at elev. 42^o



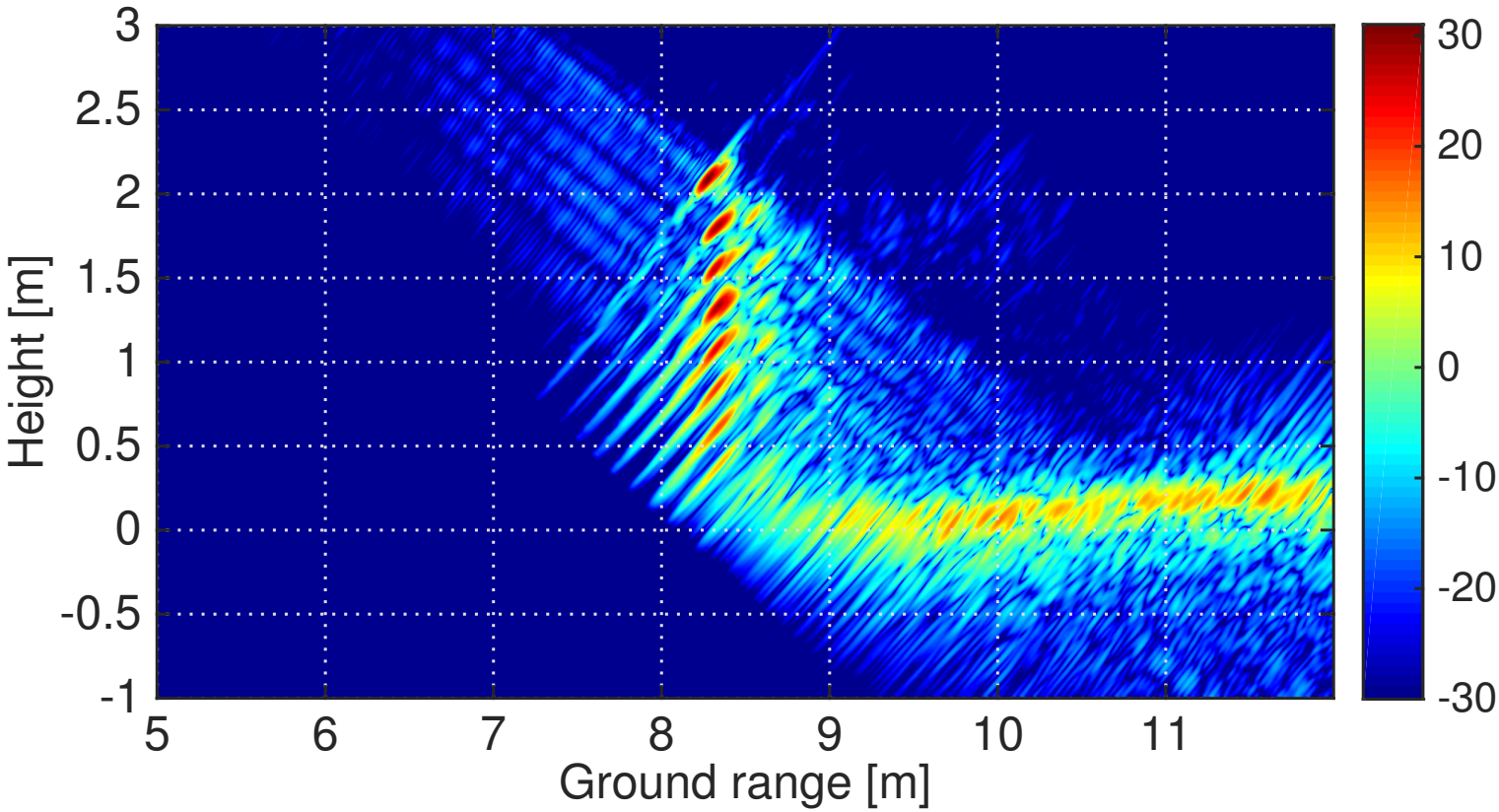
Tomographic focusing at elev. 45^o



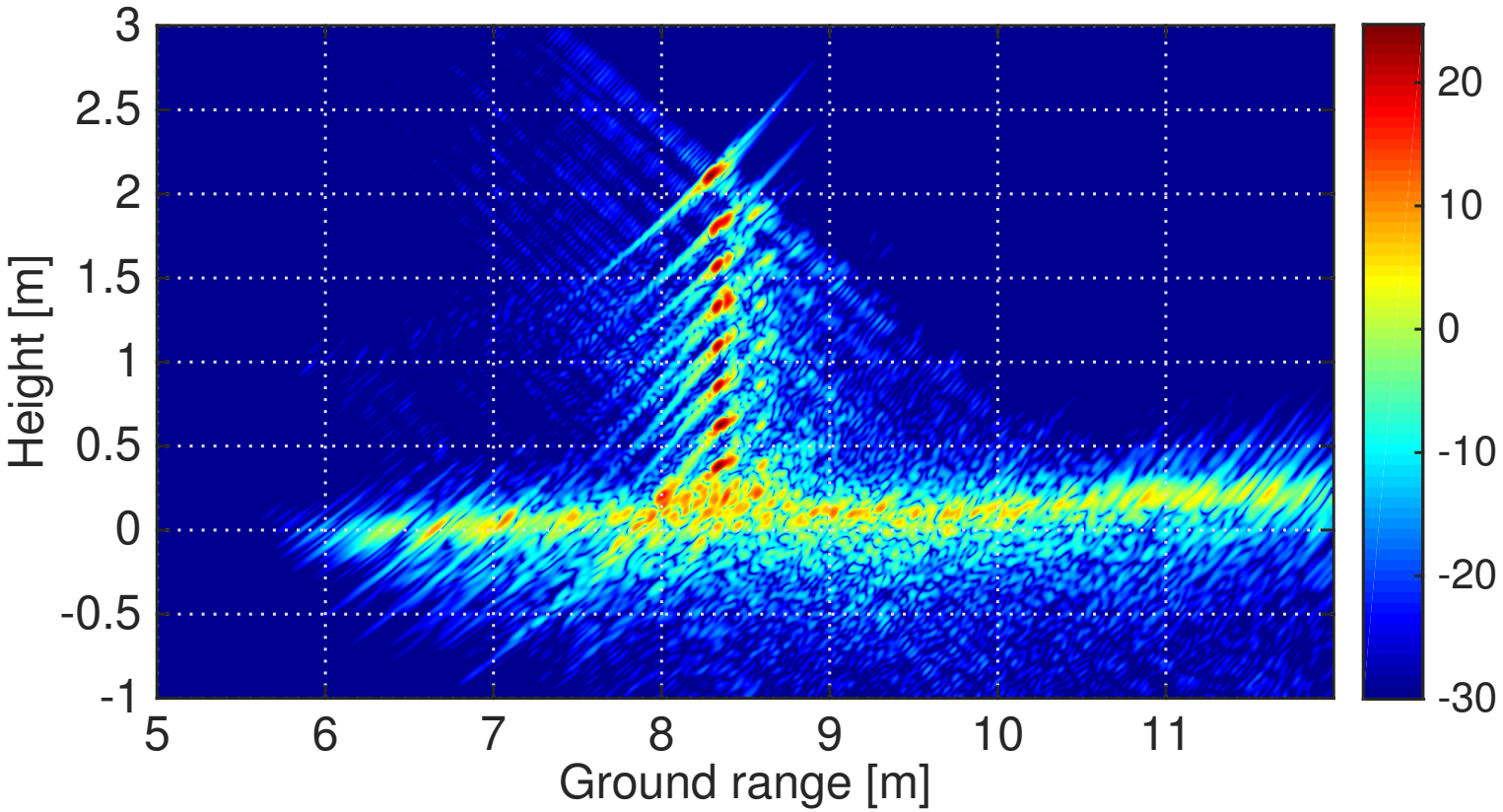
Tomographic focusing at elev. 48^o



Tomographic focusing at elev. 51^o



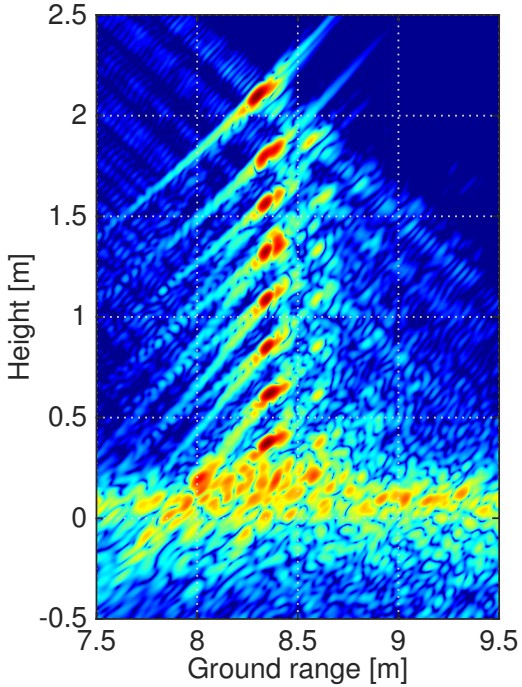
Tomogr. focusing: coherent comb. of tomograms

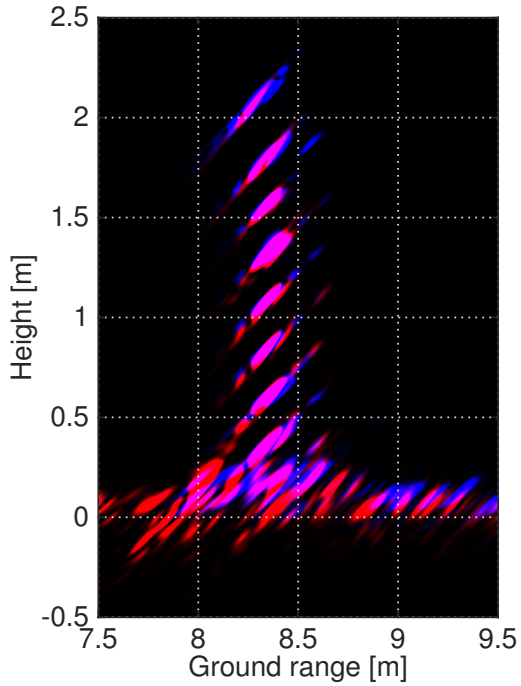


Discussion: generation of additional looks

- Additional looks can be obtained by:
  1. Splitting the range spectrum.
  2. Spatial averaging along ground range.
  3. Spatial averaging of a set of measurements taken at different azimuth angles.
     $\Rightarrow$ Introduces additional complications since for non-zero azimuth angles the synthetic aperture does not lie in a vertical plane.
  4. Moving the SnowScat antenna also in azimuth (2-D synthetic aperture in elevation and azimuth).
     $\Rightarrow$ Preferred option for optimal tomographic processing.

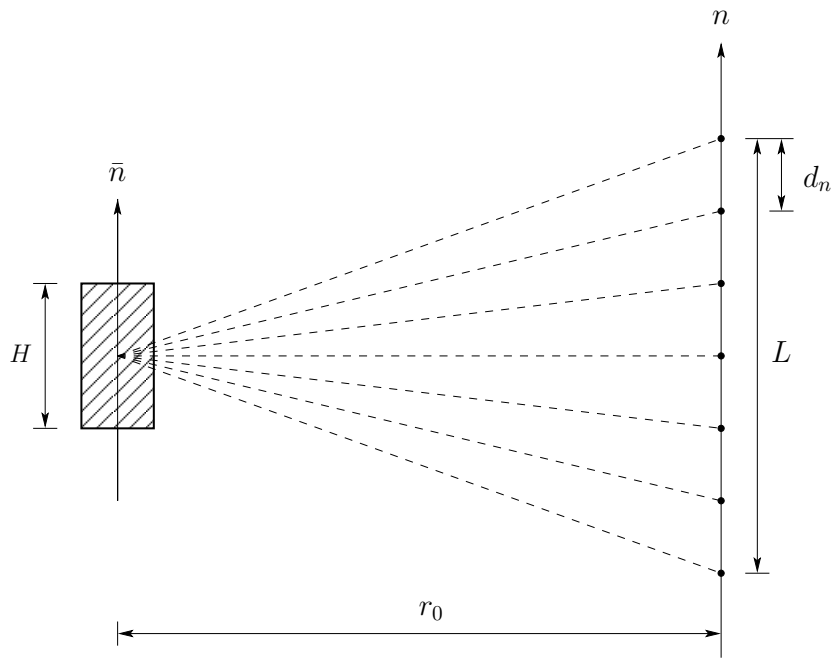
Subaperture tomograms





- Two "subaperture tomograms"
- First 20 samples (red) and the last 20 samples (blue)
- $\Rightarrow$ Moving phase centre location of the specular reflection point on the spheres as a function of the angle of incidence.

Resolution and sampling requirements



Tomographic imaging geometry. Volume is illuminated from different positions along a synthetic aperture in normal direction *n*.

Resolution ("stripmap-mode"):

$$\delta_n = \frac{2\pi}{K_{nr} \cdot L} = \frac{2\pi}{\frac{2 \cdot 2\pi}{r_0 \lambda} \cdot L} = \frac{\lambda r_0}{2L} .$$

Volume height H (in elevation direction) that can be reconstructed unambiguously:

$$d_n(\bar{n}_0 = H) \leq \frac{\lambda r_0}{2H}$$

Simplified Block Diagram of SnowScat Hardware

- Stepped-frequency, continuous-wave (SFCW) radar
- Tuneable bandwidth, frequency steps, etc.
- Settings for tomographic profiling:

$$f_{start} = 9.199984 GHz$$

$$\Delta f = 6.144 MHz$$

$$n_{f.steps} = 1400$$

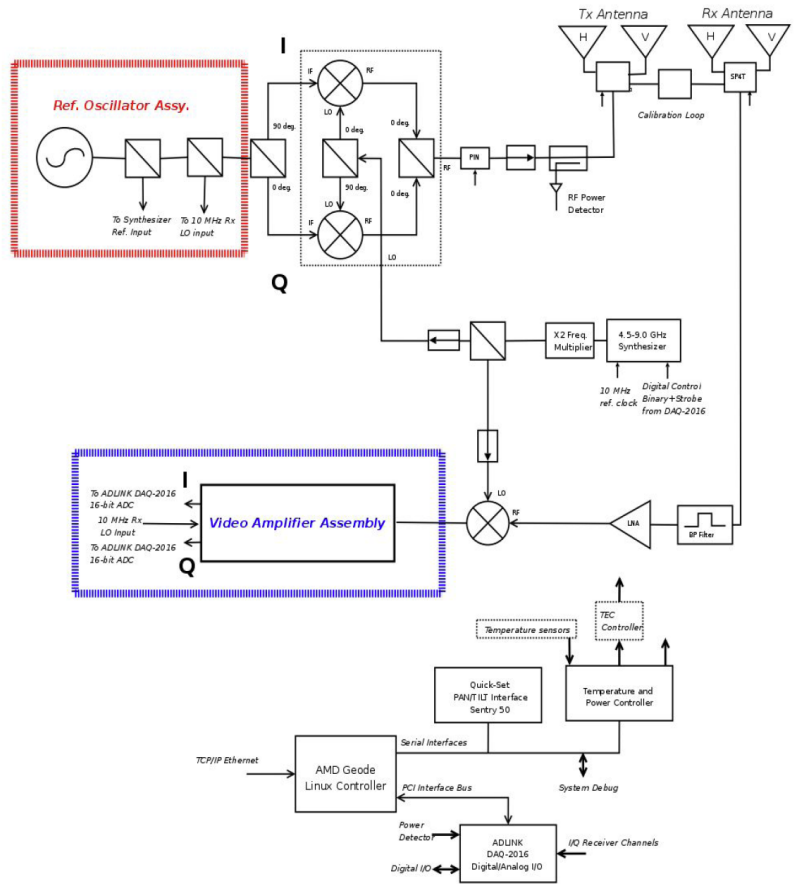
$$\rightarrow R_{unamb} = \frac{c}{2\Delta f} \approx 24.3 m$$

- Max. bandwidth:

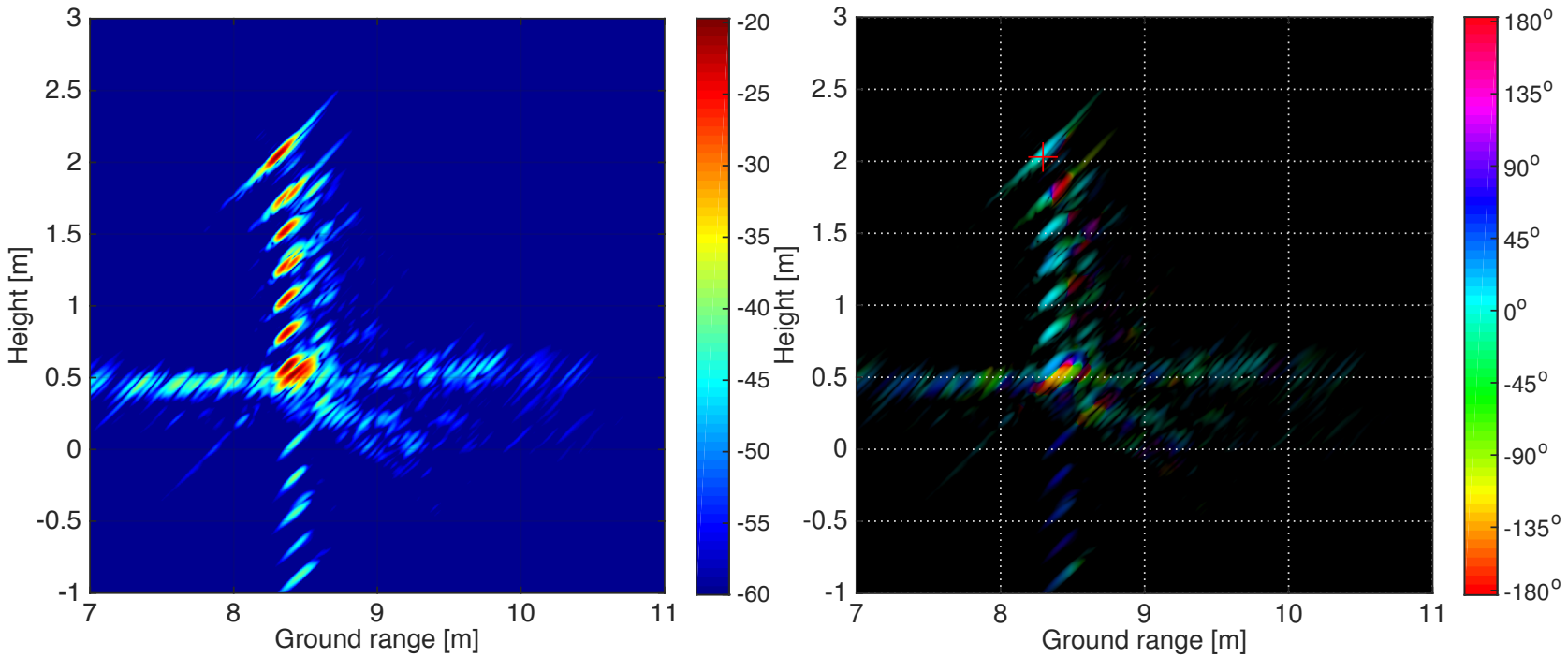
$$B = n_{f.steps}\Delta f = 8.6016 GHz$$

- Nominal range resolution:

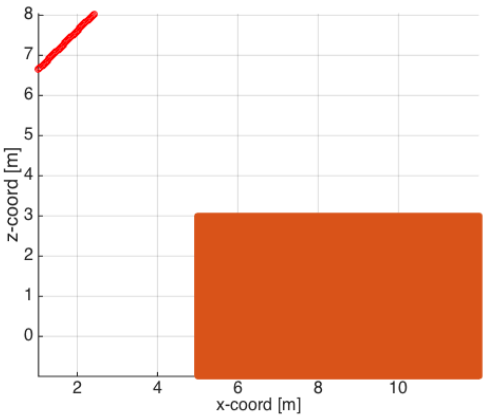
$$\rightarrow \delta R = \frac{c}{2B} = 1.73 cm!$$

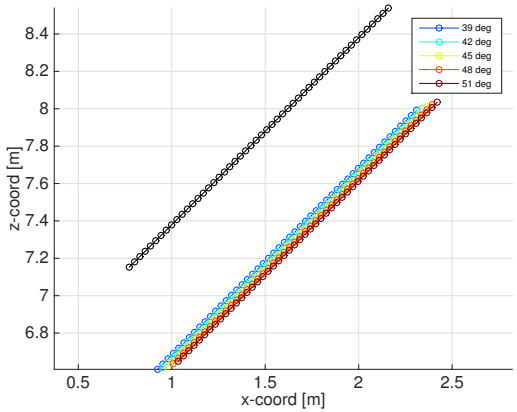


Special case: data acquisition under **melted snow surface condition**.

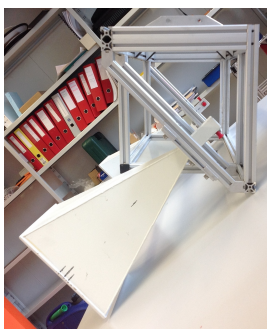


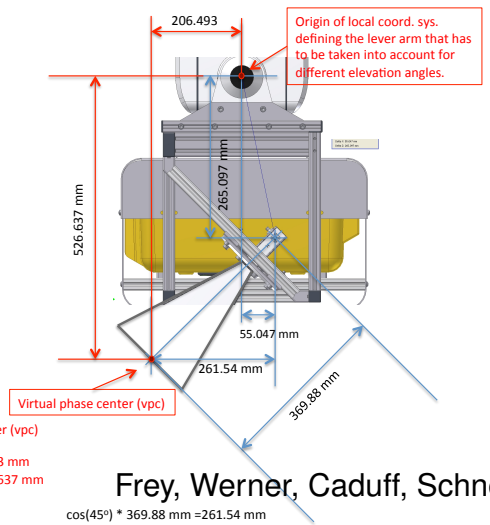
Acquisition geometry and antenna phase center locations for tomography test





SnowScat Antenna / Antenna mount
Physical dimensions (3)





Local coordinates of virtual phase center (vpc)

X_vpc = 55.047 - 261.54 mm = -206.493 mm
Y_vpc = -265.097 - 261.54 mm = -526.637 mm

cos(45°) * 369.88 mm =261.54 mm